Archives of Virology (2020) 165:2561–2587
https://doi.org/10.1007/s00705-020-04789-y

ORIGINAL ARTICLE

Inhibition of orf virus replication in goat skin fibroblast cells by the HSPA1B protein, as demonstrated by iTRAQ-based quantitative proteome analysis

Jun-hong Hao[1] · Han-jin Kong[1] · Ming-hao Yan[1] · Chao-chao Shen[1] · Guo-wei Xu[1] · Da-jun Zhang[1] · Ke-shan Zhang[1] · Hai-xue Zheng[1] · Xiang-tao Liu[1]

Received: 8 March 2020 / Accepted: 26 July 2020 / Published online: 2 September 2020

Abstract

Orf virus (ORFV) infects sheep and goat tissues, resulting in severe proliferative lesions. To analyze cellular protein expression in ORFV-infected goat skin fibroblast (GSF) cells, we used two-dimensional liquid chromatography-tandem mass spectrometry coupled with isobaric tags for relative and absolute quantification (iTRAQ). The proteomics approach was used along with quantitative reverse transcription polymerase chain reaction (RT-qPCR) to detect differentially expressed proteins in ORFV-infected GSF cells and mock-infected GSF cells. A total of 282 differentially expressed proteins were identified. It was found that 222 host proteins were upregulated and 60 were downregulated following viral infection. We confirmed that these proteins were differentially expressed and found that heat shock 70-kDa protein 1B (HSPA1B) was differentially expressed and localized in the cytoplasm. It was also noted that HSPA1B caused inhibition of viral proliferation, in the middle and late stages of viral infection. The differentially expressed proteins were associated with the biological processes of viral binding, cell structure, signal transduction, cell adhesion, and cell proliferation.

Introduction

Orf, which is caused by orf virus (ORFV), is one of the most widespread viral diseases worldwide. Although ORFV mainly infects sheep and goats, it can also infect other ruminants and other mammals [18]. Genes involved in virulence and pathogenesis are distributed in the ITR regions of the ORFV genome. The virus encodes involved in immunomodulation, including viral-interleukin 10 (vIL-10, ORFV127), vascular endothelial growth factor (VEGF, ORFV132), orf virus interferon resistance protein (OVIFNR, ORFV020), chemokine binding protein (CBP, ORFV112), granulocyte–macrophage colony-stimulating factor/interleukin-2 (GM-CSF/IL-2) inhibitory protein (GIF, ORFV117), nuclear factor kappa B (NF-κB) inhibitory protein (ORFV125), and deoxyuridine 5′-triphosphate pyrophosphatase (dUTPase, ORFV007) [38].

Like other poxviruses, ORFV encodes a range of molecules that play vital roles in immune evasion by the production of anti-inflammatory proteins [13]. These proteins, which are mainly involved in the interaction with host defense mechanisms, include OVIFNR, GIF, vIL-10, and VEGF. A number of these proteins are orthologues of known mammalian proteins, whereas others do not appear to have mammalian counterparts [7, 11–13]. ORFV encodes GIF, which is a novel secreted inhibitor of the cytokines GM-CSF and IL-2 [7]. GIF co-localizes with ORFV in infected epidermal cells, as detected by immunohistochemistry (IHC) [13]. Both ORFV and ovine IL-10 (vIL-10 and ovIL-10) inhibit production of tumor necrosis factor-α (TNF-α) and IL-8 from macrophages and keratinocytes as well as production of interferon gamma (IFN-γ) from activated lymphocytes [10]. The viral VEGF is important for virulence [25, 34, 40]. It is mitogenic to endothelial cells and promotes angiogenesis in the underlying dermis as well as proliferation of epidermal cells and activation of VEGF receptors. Aside from an array of immunomodulatory factors produced by ORFV, poxviruses also produced a class

Handling Editor: William G Dundon.

✉ Ke-shan Zhang
vetzks009@163.com

[1] State Key Laboratory of Veterinary Etiological Biology, National Foot-and-Mouth Disease Reference Laboratory, Lanzhou Veterinary Research Institute of Chinese Academy of Agriculture Science, No. 1, Xujiaping, Lanzhou 730046, Gansu, People's Republic of China

of proteins, namely ankyrin (ANK) repeat proteins [28], which can also promote viral survival. A proteomic analysis of host cellular responses to viral infection may provide new insights into the cellular mechanisms involved in viral pathogenesis.

The isobaric tag for relative and absolute quantitation (iTRAQ) technique allows comprehensive, comparative, and quantitative determination of protein expression [33]. This technique has been extensively applied to proteome analysis [3, 14, 15, 33, 39]. iTRAQ simultaneously identifies and quantifies peptides by measuring peak intensities of reporter ions using tandem mass spectroscopy (MS/MS) and has been developed to identify biomarkers for various viral diseases [2, 41]. This method has been widely utilized to study the mechanisms of viral infection through the comparative analysis of cellular protein profiles. In the present study, a comparative iTRAQ-based proteomic analysis was conducted to analyze the changes in cellular proteins of goat skin fibroblast (GSF) cells exposed to ORFV in vitro at specific time points. The experiments were performed to investigate functional changes occurring in GSF cells infected by ORFV. This is the first study on the interactions of ORFV with its host using a proteomics approach. The purpose of the present study was to investigate the adaptability and proliferation of ORFV in goat skin fibroblasts. Hence, the iTRAQ-2D-LC–MS/MS technology was used to analyze proteomic changes in ORFV-infected GSF cells. Quantitative reverse transcription polymerase chain reaction (RT-qPCR) and other methods were applied to identify differentially expressed proteins and to further analyze and confirm the function of the differentially expressed proteins and heat shock 70-kDa protein 1B (HSPA1B) in ORFV-infected host cells. These data provide a foundation for mapping of gene regulatory networks that are affected by ORFV infection.

Materials and methods

Cell culture and virus infection

GSF cells were purchased from the Kunming Institute of Zoology, Chinese Academy of Sciences (Kunming, China) and cultured in complete Dulbecco's modified Eagle's medium (DMEM; HyClone Laboratories Inc., Logan, UT, USA), containing 10% fetal bovine serum (FBS; Gibco, New York, NY, USA) in an incubator with 5% CO_2. The GSF cell line was tested for mycoplasma contamination, which showed an appropriate microscopic morphology. ORFV was isolated and stored in our laboratory for further experiments. ORFV was passaged continuously for 15 generations on GSFs, virus samples were selected after the 1st, 5th, 10th, and 15th generations, and the viral genome was extracted for B2L gene detection. A 1137-bp fragment of the genome corresponding to the ORFV B2L gene was sequenced, and found to be identical to an ORFV B2L gene sequence published in the Gene Bank database (GU320351).

Growth curve of ORFV in GSF cells

To analyze the growth of ORFV in GSF cells, the cells were infected at an MOI of 0.1 in a 24-well plate, and uninfected cells served as a control. Samples were collected at 2, 12, 18, 24, 36, 48, and 60 h postinfection. The ORFV copy number was estimated using RT-qPCR.

Sample preparation

The cultured GSF cells were divided into an experimental group and a control group. When the cells reached about 80% confluency, 500 µL of ORFV suspension (MOI, 0.1) was added to the cells in the experimental group, and DMEM was added to the cells in the control group. The cells were incubated for 1 h and washed three times with phosphate-buffered saline (PBS), and DMEM medium containing 2% FBS was added. The cells were collected and protein samples were prepared after 35 h. The culture medium was discarded, and the cells were washed three times with cold PBS, scraped with a cell scraper, and collected in a centrifuge tube. The cells were pelleted by centrifugation at 2000 rpm for 3 min, resuspended and washed two times, and the final cell pellet was stored at -80 °C for further experiments.

Protein extraction

Five hundred µL of protein lysate was added to the sample and lysed on ice. Phenylmethylsulfonyl fluoride (PMSF) and dithiothreitol (DTT) with final concentrations of 1 and 10 mM, respectively, were added. After sonication in an ice bath for 15 min, the sample was centrifuged, and the supernatant was treated at 56 °C for 1 h to reduce disulfide bonds. Next, iodoacetamide (IAM) was added to a final concentration of 55 mM, and the sample was kept in the dark for 45 min to block cysteine alkylation. An appropriate amount of cold acetone was added, and the sample was stored at -20 °C for 2 h. The sample centrifuged at 14,000 rpm for 20 min, the supernatant was discarded, and 200 µl of 0.5 mM tetraethylammonium borohydride (TEAB) was added to the pellet, which was sonicated for 15 min, and centrifuged at 14,000 rpm for 20 min.

Protein concentration measurement

Protein quantification was done by the Bradford method, using prepare a standard curve made from series of dilutions

of bovine serum albumin (BSA) and measuring absorbance at 595 nm.

Protein digestion and iTRAQ labeling

One hundred μg of protein was trypsinized for 12 h. After enzymatic digestion, the peptide was dried using a vacuum centrifugal pump and reconstituted with 0.5 M TEAB. iTRAQ labeling was done according to the manufacturer's instructions. Labeling reagent 116 was used to label the experimental group, and labeling reagent 119 was used to label the control group. After incubation at room temperature for 2 h, the labeled peptides of each group were mixed and separated by liquid-phase chromatography using a strong cation-exchange (SCX) column.

SCX chromatography

An LC-20AB high-performance liquid chromatography (HPLC) pump system (Shimadzu, Tokyo, Japan) and a 4.6 × 250-mm separation column were used for liquid-phase separation of the samples. The mixed peptides were labeled were reconstituted and 4 ml of buffer A. Gradient elution was performed at a rate of 1 ml/min. The first elution was performed with buffer A for 10 min, which was gradually mixed with 5–35% buffer B for 11 min, and finally mixed with 35–80% buffer B and eluted for 1 min. The entire elution process was monitored by measuring the absorbance at 214 nm, and 20 components were eventually selected. Each component was desalted separately using a Strata-X C18 column (Phenomenex, Torrance, CA, USA) and then freeze-dried.

Capillary HPLC

The concentration of each component that was adjusted to about 0.5 μg/μl with buffer C and centrifuged at 20,000 rpm for 10 min to remove insoluble matter. Eight microliters of each component (about 4 μg of protein) was separated using a Shimadzu LC-20AD HPLC system (Shimadzu, Tokyo, Japan). The column included a trap column and an analytical column. The separation parameters were as follows: injection for 4 min at a flow rate of 8 nL/min, washing at a flow rate of 300 nL/min for 40 min, washing with gradient buffer D from 2–35% and then from 35–80%, and washing with 80% buffer D for 4 min and buffer C for 1 min.

Electrospray ionization mass spectrometry (ESI-MS)

The peptides were separated using a Q-Exactive mass spectrometer. The primary MS resolution was set to 70,000 full width at half maximum (FWHM). The peptides were screened using a high-energy collision mode with a collision energy of 27 (± 12). Secondary fragments were detected in Orbi with a resolution of 17,500 FWHM. In addition, 15 secondary spectra were plotted for primary precursor ions with peak intensities in excess of 20,000, and primary and secondary scanning was performed. Scanned mass-to-charge ratios ranged from 350 to 2000 Da.

MS data analysis

The original mass spectrum file was converted to MGF format. The quantitative data were analyzed by iTRAQ Result Multiple File Distiller, and the MGF file was used as an original file with Mascot2.3.02 protein identification software. A selected sheep genome annotation database (22134 sequences) and ORFV virus from the NCBI database (150 sequences) were used for searching and combined with the quantitative results.

Bioinformatics analysis

Functional annotation, subcellular localization, and metabolic pathway analysis of the identified differentially expressed proteins were carried out. The hypergeometric test was used to find Gene Ontology (GO) entries that were enriched compared with other proteins. These differentially expressed proteins were compared with the Clusters of Orthologous Groups of proteins (COG) database to predict the possible functions of these proteins and perform statistical analysis on their functional classification.

RT-qPCR

Specific primers (Table 1) were designed to amplify various target genes simultaneously according to the corresponding gene sequences of MS/MS-identified proteins, and the available genetic information was deposited in the GenBank database. The analysis was conducted using Lasergene sequence analysis software (DNASTAR, Inc., Madison, WI, USA). GSF monolayers were inoculated with ORFV for 35 h and washed three times with ice-cold PBS. They were then harvested by centrifugation at 1,000 rpm for 10 min. Total cellular RNA was extracted using an RNeasy Mini Kit (QIAGEN GmbH, Hilden, Germany) according to the manufacturer's protocol. The RNA concentration was measured using a spectrophotometer (260/280 nm). RT-qPCR was performed using an Mx3005P Real-Time PCR System (Agilent Technologies, Inc., Santa Clara, CA, USA). A reverse transcription step was first performed at 42 °C for 5 min to make cDNA from total RNA. The PCR procedure consisted of a denaturation step at 95 °C for 10 s, followed by 40 cycles of amplification, each consisting of an extra denaturation step at 95 °C for 5 s and a primer annealing step at 60 °C for 34 s. Melting curves were plotted, and

Table 1 Primers used for the goat target genes based on the corresponding gene sequences of the identified proteins. Specific primers were designed to simultaneously amplify various target genes according to the corresponding gene sequences of identified proteins, and the available gene information was deposited in the GenBank database

Gene name	Primer sequence (5′ -3′)
BCLF1	F: AAGATACATTTGAACACGACCCG
	R: ATCCATTTCCAACAGAACCAGAC
PARP1	F: TCGGGCTCGTGGACATCGT
	R: GGCATCTGCTCCAGTTTGT
COR1B	F: TTGCCCTTCTACGACCCTGAT
	R: GGCTCCTTGCTGGTGAATGTA
MAP4	F: GGCTCCCAATGCTTCTGC
	R: CCCGTAGGCGGTTTCTGT
6PGD	F: ATGGCTTTGTGGTCTGTGC
	R: CCGTCTCATGGTATCCCTGTAT
G3P	F: AAGTTCCACGGCACAGTCA
	R: TGGTTCACGCCCATCACAA
SC24D	F: GCTATTATGCGGGTTCG
	R: ATCAAGGCTCCAGTGTC
ZN207	F: TACCTGGGAGAACAGACAT
	R: GCTGCGGTTGAAATGAAGT
FIS1	F: ACAGAGCCGCAGAACAACCA
	R: TCCGATGAGTCCAGCCAGTC
CDV3	F: CCTCCTGCTCCAGTAGTTGTT
	R: TTGTGGTGCTTTCCTTGTTGT
VMA5A	F: CCAACTGCTCCTTGAGTCCTA
	R: AGCTTCTCCCATCTCCACGA
PSME2	F: CCCACCCAAGGATGATGAGAT
	R: GAAAGCCGCACTTAGGGACTG
ACTB	F: ACACGGTGCCCATCTACGA
	R: TTGATGTCACGGACGATTTC
GAPDH	F: AAGTTCCACGGCACAGTCA
	R: TGGTTCACGCCCATCACAA
B2L	F: GGGGCGGCGTATTCTTCT
	R: GCTGTTCTTGGCGTTCTCG
HSPA1B	F: GGGAGGACTTCGACAACAGG
	R: GACAAGGTTCTCTTGGCCCG

quantitative analysis of the data was conducted using the 7500 Fast System SDS 1.3.1 software (Applied Biosystems, Foster City, CA, USA). Mock-infected GSF cells were used as a control. The RT-PCR products were analyzed by electrophoresis in a 2% agarose gel.

Subcellular localization of HSPA1B

Cells were seeded into 6-well plates and cultured overnight in DMEM in the presence of 10% FBS. The transfection mixture, which contained 2.0 μg of plasmid DNA and 6 μL of transfection reagent (Invitrogen, Carlsbad, CA, USA) in 100 μL of serum-free DMEM, was mixed for 20 min at room temperature and subsequently added to each well with complete medium for 24 h. The cells were evaluated for protein expression by fluorescence microscopy at 24–48 h post-transfection and then were fixed by conventional methods and stained with 4′,6-diamidino-2-phenylindole (DAPI). The cellular distribution of HSPA1B was analyzed by confocal laser scanning microscopy (CLSM).

Measurement of the effect of HSPA1B on ORFV replication

In order to examine the influence of HSPA1B on the proliferation of ORFV, GSF cells were transiently transfected with pEFGP-HSPA1B plasmids as described previously. Subsequently, the cells were infected with ORFV at an MOI of 0.1. After incubation for 1 h, the cells were washed three times with PBS and DMEM containing 2% FBS was added. The cultured cells were collected at 15, 24, and 36 h postinfection and the viral DNA was quantitated using RT-qPCR.

RNA interference

Small interfering RNA (siRNA) was chemically synthesized by Gene Pharma (Shanghai, China). The knockdown of endogenous HSPA1B was carried out by transfection of GSF cells with HSPA1B siRNA (517) (5′- UUUGUAGCU CACCUGCACCTT-3′), HSPA1B siRNA (1258) (5′- GUU GAAGAAGUCCUGCAGCTT-3′), and HSPA1B siRNA (1486) (5′- GUAGGUGGUGAAGAUCUGCTT-3′) using Lipofectamine 2000. Nontargeting siRNA (NC siRNA) was used as a negative control.

Western blot

For Western blotting, target proteins were resolved by SDS-PAGE and transferred to an Immobilon-P membrane (Millipore). The membrane was blocked and incubated with appropriate primary antibodies and secondary antibodies. Antibody-antigen complexes were visualized using enhanced chemiluminescence detection reagents (Thermo) [42]. Mouse anti-HSPA1B anti-β-actin antibodies were purchased from Abbkine. Mouse anti-B2L antibody was obtained from the Lanzhou Veterinary Research Institute.

Results

Growth of ORFV in GSF cells

In order to assess the growth of ORFV in GSF cells, a one-step growth curve was carried out using RT-qPCR. ORFV was adapted to GSF infection by passaging for 15

generations. At different time points, the supernatants and the cells were collected, and the copy number of viral DNA was determined by RT-qPCR to prepare a one-step growth curve. The results indicated that the intracellular viral DNA content increased from 2 to 36 h postinfection and reached the highest level at 36 h. The extracellular viral DNA content gradually increased (Fig. 1A), while the intracellular viral DNA content decreased during this time period, and the extracellular viral DNA content increased to form an S-shaped curve. The eclipse phase was from 0 to 12 h postinfection, during which the viral content remained at a low level. The logarithmic phase was from 12 to 48 h, and the viral DNA content increased, reaching a peak at 48 h, slowing from 48 to 60 h postinfection, and gradually reaching a plateau (Fig. 1B).

Kinetics of ORFV-induced cytopathology in cultured GSF cells

One of the key parameters for determining virus-induced alterations is the length of time until a cytopathic effect (CPE) is observed in the model system. GSF cells were infected with ORFV at an MOI of approximately 0.1, and monitored for cell viability and CPE. As shown in Fig. 2, the cells infected with ORFV that were cultured for less than 24 h demonstrated no detectable CPE (Fig. 2A-B). At 24 h postinfection, a small number of cells began to swell and had a round shape (Fig. 2C-D). At 60 h, the cells detached from the plate (Fig. 2E) and were completely destroyed after 72 h postinfection (Fig. 2F-G).

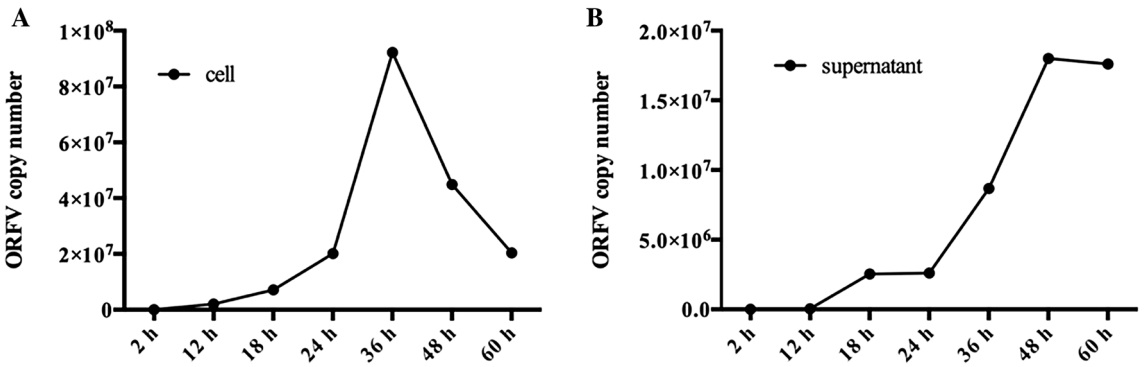

Fig. 1 One-step growth curve of ORFV infection in GSF cells. GSF cells were infected with ORFV at an MOI of 0.1 and cell supernatants and infected cells were collected at 2, 12, 18, 24, 36, 48, and 60 h postinfection. RT-qPCR was used to make a one-step growth curve to measure the copy number of the intracellular virus (Fig. 1A) and extracellular virus (Fig. 1B)

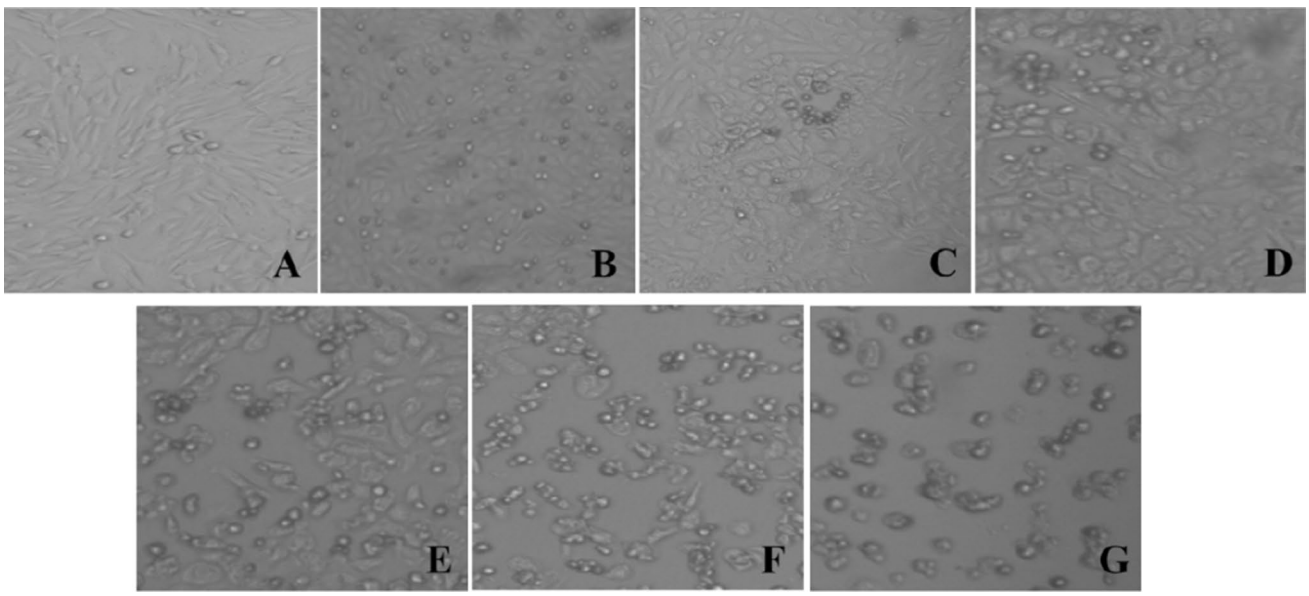

Fig. 2 Kinetics of the ORFV-induced cytopathic effect (CPE) in GSF cells. Cells at about 80% confluency were infected with ORFV at an MOI of 0.1 or mock infected, and DMEM was added to the cells in the control group, and after 1 h, the cells were washed three times with PBS, and DMEM 2% FBS was added. Morphological changes were then examined at different time points

Differentially expressed proteins analyzed by iTRAQ-coupled 2D LC/MS-MS

The cellular proteins in ORFV-infected and mock-infected GSF cells were extracted for iTRAQ analysis. In total, 10,630 peptides and 2,776 proteins were detected. Of these, 282 proteins were found to be differentially expressed in ORFV-infected GSF cells compared with the mock-infected GSF cells, including 222 significantly upregulated proteins and 60 significantly downregulated proteins. The upregulated proteins are listed in Table 2, and the downregulated proteins are listed in Table 3. Three proteins that are involved in cell killing showed altered expression levels. The levels of CXCL6, IFNG (interferon gamma [IFNγ]), and ALBU increased after infection. In addition, 28 proteins involved in cell proliferation exhibited differential expression. NFIP1, IFNG, TKT, CD9, BAK, HS71B, CSK2B, NPM, HDGF, PA2G4, CDV3, RL23A, THIO, MCM7, CXCL6, YBOX1, RS4X, CYR61, HMOX1, APOD, TANA, RS6, and PAI1 were upregulated, while CAV1, GBG2, ZPR1, MK01, and LAMB2 were downregulated. CXCL6 and IFNG are associated with pathways involved in apoptosis [5, 22] and proliferation [23, 29]. Changes in the levels of biological adhesion proteins were also detected, including PAI1, APOD, CTGF, ADAM9, EZRI, CYR61, CD9, and TKT, which were upregulated, and TBCD, VINC, CO3A1, 2AAA, LAMB2, and PARVA were downregulated. The abundance of the 70-kDa heat shock proteins (HSPs) HSPA6 and HSPA1B increased after infection. Moreover, several ribosomal proteins, including RPS6, RPS17, RPS3, RPS21, RPS18, RPS3A, Rps16, Rps8, RPS4X, Rps23, RPS2, RPS19, RPS12, Rps13, and RPS20 were upregulated (Table 2). However, no ribosomal proteins were downregulated after infection (Table 3).

Functional classification of differentially expressed proteins

To understand the implications of the cellular responses to ORFV infection, these proteins were categorized into three main types using the UniProt Knowledgebase (Swiss-Prot/TrEMBL) and the GO databases: cellular components, metabolic functions, and biological processes. Cell component ontology refers to subcellular structures, locations, and macromolecular complexes, such as nucleoli, telomeres, and complexes that recognize initiation. Cellular-component-based enrichment analysis identified differentially expressed proteins that are well distributed in cell components (Fig. 3A) and are mainly involved in morphogenesis, protein synthesis, metabolism, the stress response, the ubiquitin–proteasome pathway, cellular processes, metabolic processes, biological regulation, and response to stimuli. Molecular function ontology refers to the function of an individual gene product, such as carbohydrate binding or ATP hydrolase activity. Molecular-function-based enrichment analysis demonstrated that binding, catalytic activity, structural molecule activity, and enzymatic regulation were influenced by viral infection (Fig. 3B). Biological processes ontology refers to the ordered combination of molecular functions to achieve a wider range of biological functions, such as mitosis or purine metabolism. Enrichment analysis using biological processes indicated that viral infection mainly affected cellular and metabolic processes (Fig. 3C). A protein may have multiple GO annotations. To determine which biological functions were associated with differentially expressed proteins, a significant enrichment analysis of GO functions was carried out on these differentially expressed proteins. The results revealed that these differentially expressed proteins were mainly localized in the cytoplasm, ribosomes and the nucleus (Fig. 3D). Molecular enrichment analysis showed that these differentially expressed proteins included proteins with nucleic acid binding activity, threonine peptidase activity, and growth factor binding activity (Fig. 3E). Gene set enrichment analysis revealed that these differentially expressed proteins were mainly involved in the initiation and termination of transcription, which are related to virus replication and signal transduction processes (Fig. 3F). The identified differentially expressed proteins were compared with the COG database, and possible functions of these proteins were predicted. COG annotation classification indicated that the differentially expressed proteins were mainly involved in functions such as post-translational modification, protein folding, molecular chaperones, translation, ribosome structure and biosynthesis, energy generation and conversion, and signal transduction (Fig. 3G).

Confirmation of proteomic data by RT-qPCR

Changes in transcription of 12 genes selected from the differentially expressed proteins were analyzed by quantifying their mRNA transcripts. The "β-actin" (ACTB) gene was used as a control. The pattern of differences in mRNA abundance for these genes between infected and control GSF cells was similar to the pattern observed for the corresponding proteins based on LC–MS/MS data. As shown in Fig. 4, the abundance of BCLF1, MAP4, 6PGD, G3P, ZN207, and CDV3 mRNA increased. The SC24D, FIS1, COR1B, and PSME2 genes were downregulated, whereas the PARP1 gene was upregulated. An inconsistency between the RT-qPCR data and the LC–MS/MS data was observed for VMA5A, which was downregulated in the RT-qPCR analysis and upregulated in the LC–MS/MS analysis. This inconsistency might have been due to post-translational modifications, such as methylation, phosphorylation, or acetylation, or to differences in protein degradation rates for unknown reasons. These data provide transcriptional

Table 2 Upregulated proteins identified by iTRAQ analysis of ORFV-infected GSF cells. These proteins had expression ratios > 1.2 relative to the control group at the same time postinfection

Group ID	Accession no	Score	%Cov (95%)	Peptide (95%)	Unique peptide	vorfM_116: CK_119	Protein abbreviation	Protein description	COG function description
1	1::GOAT_ENSP00000369757	185	21.1	4	3	1.263	RPS6	40S ribosomal protein S6	Ribosomal protein S6E (S10)
2	1::GOAT_ENSBTAP00000024092	82	14.2	5	5	1.234	AHCY	Adenosylhomocysteinase	S-adenosylhomocysteine hydrolase
3	1::GOAT_ENSBTAP00000016634	130	4.2	1	1	1.472	IFNG	Interferon gamma	-
4	1::GOAT_ENSBTAP00000029157	45	2.8	1	1	1.319	FAM98B	Protein FAM98B	-
5	1::GOAT_ENSBTAP00000000814	58	25.2	2	2	1.219	RPS17	40S ribosomal protein S17	Ribosomal protein S17E
6	1::GOAT_ENSBTAP00000019643	61	25.1	4	4	1.392	CD9	CD9 antigen	-
7	1::GOAT_ENSP00000410059	306	12.3	4	4	1.347	EEF1D	Elongation factor 1-delta	Translation elongation factor EF-1beta
8	1::GOAT_ENSBTAP00000015277	190	9.3	7	7	1.247	PYGL	Glycogen phosphorylase, liver form	Glucan phosphorylase
9	1::GOAT_ENSP00000278572	244	39.9	8	8	1.337	RPS3	40S ribosomal protein S3	Ribosomal protein S3
10	1::GOAT_ENSP00000325376	361	12.7	9	9	1.343	HNRNPM	Heterogeneous nuclear ribonucleoprotein M	RNA-binding proteins (RRM domain)
11	1::GOAT_ENSBTAP00000002587	48	16.1	3	3	1.231	SNRNP70	U1 small nuclear ribonucleoprotein 70 kDa	RNA-binding proteins (RRM domain)
12	1::GOAT_ENSP00000391481	131	14.7	5	5	1.267	TKT	Transketolase	Transketolase
13	1::GOAT_ENSP00000408263	379	41.7	13	13	1.226	SELENBP1	Selenium-binding protein 1	-
14	1::GOAT_ENSP00000313007	266	12.8	7	4	1.398	PABPC1	Polyadenylate-binding protein 1	RNA-binding proteins (RRM domain)
15	1::GOAT_ENSBTAP00000027991	166	16.3	9	8	1.261	Khsrp	Far upstream element-binding protein 2	-
16	1::GOAT_ENSP00000264073	94	18.4	5	5	1.291	ELAVL1	ELAV-like protein 1	RNA-binding proteins (RRM domain)
17	1::GOAT_ENSBTAP00000041860	241	34	3	3	1.246	TXN	Thioredoxin	Thiol-disulfide isomerase and thioredoxins
18	1::GOAT_ENSBTAP00000002045	71	18.1	5	5	1.317	MESDC2	LDLR chaperone MESD	-
19	1::GOAT_ENSBTAP00000022576	208	20.5	3	1	1.352	h2afv	Histone H2A.V	Histone H2A
20	1::GOAT_ENSP00000367550	1243	19.1	8	2	1.335	TPM2	Tropomyosin beta chain	-
21	1::GOAT_ENSBTAP00000027713	50	12.3	1	1	2.11	RPS21	40S ribosomal protein S21	-
22	1::GOAT_ENSBTAP00000023094	167	20.6	3	2	1.974	YBX1	Nuclease-sensitive element-binding protein 1	Cold shock proteins
23	1::GOAT_ENSBTAP00000021345	19	0.3	1	1	1.418	RGPD5	RANBP2-like and GRIP domain-containing protein 5/6	-
24	1::GOAT_ENSP00000225972	188	19	5	5	1.332	LRRC59	Leucine-rich repeat-containing protein 59	Leucine-rich repeat (LRR) protein
25	1::GOAT_ENSBTAP00000000630	63	16.6	4	4	1.32	AKR1A1	Alcohol dehydrogenase [NADP(+)]	Aldo/keto reductases, related to diketogulonate reductase

Table 2 (continued)

Group ID	Accession no	Score	%Cov (95%)	Peptide (95%)	Unique peptide	vorfM_116: CK_119	Protein abbreviation	Protein description	COG function description
26	1::GOAT_ENSP00000279230	75	0.7	1	1	1.578	PLCB3	1-phosphatidylinositol 4,5-bis-phosphate phosphodiesterase beta-3	-
27	1::GOAT_ENSBTAP00000040666	80	5.8	2	2	1.441	TOE1	Target of EGR1 protein 1	-
28	1::GOAT_ENSBTAP00000004408	113	4.9	4	4	1.24	SMARCA5	SWI/SNF-related matrix-associated actin-dependent regulator of chromatin subfamily A member 5	Superfamily II DNA/RNA helicases, SNF2 family
29	1::GOAT_ENSP00000325905	102	10.9	2	1	1.527	Srsf7	Serine/arginine-rich splicing factor 7	RNA-binding proteins (RRM domain)
30	1::GOAT_ENSBTAP00000021643	262	10.9	2	2	1.376	Snrpf	Small nuclear ribonucleoprotein F	Small nuclear ribonucleoprotein (snRNP) homolog
31	1::GOAT_ENSP00000246789	38	10	3	3	1.221	PRMT1	Protein arginine N-methyltransferase 1	SAM-dependent methyltransferases
32	1::GOAT_ENSBTAP00000029007	87	11.2	3	3	1.288	ZC3H15	Zinc finger CCCH domain-containing protein 15 SV = 1	Uncharacterized conserved protein, contains CCCH-type Zn-finger protein
33	1::GOAT_ENSP00000416110	111	13.8	3	3	1.474	RPS18	40S ribosomal protein S18	Ribosomal protein S13
34	1::GOAT_ENSP00000253024	169	6.6	3	3	1.274	TRIM28	Transcription intermediary factor 1-beta	-
35	1::GOAT_ENSP00000327539	485	25.2	8	2	1.44	HNRNPH1	Heterogeneous nuclear ribonucleoprotein H	-
36	1::GOAT_ENSBTAP00000020081	26	5.3	1	1	1.488	SGTA	Small glutamine-rich tetratricopeptide repeat-containing protein alpha	FOG: TPR repeat
37	1::GOAT_ENSP00000356420	64	7.8	3	3	1.266	UCHL5	Ubiquitin carboxyl-terminal hydrolase isozyme L5	-
38	1::GOAT_ENSP00000253332	194	6.3	6	6	1.236	AKAP12	A-kinase anchor protein 12	-
39	1::GOAT_ENSP00000296755	297	5.5	9	8	1.206	MAP1B	Microtubule-associated protein 1B	-
40	1::GOAT_ENSBTAP00000008386	137	12.2	5	5	1.771	GPI	Glucose-6-phosphate isomerase	Glucose-6-phosphate isomerase
41	1::GOAT_ENSBTAP00000012977	141	7.6	2	2	1.266	CYR61	Protein CYR61	-
42	1::GOAT_ENSBTAP00000008111	103	14.7	6	6	1.424	RBM45	RNA-binding protein 45	-
43	1::GOAT_ENSP00000346120	179	11	6	6	1.294	DDX21	Nucleolar RNA helicase 2	Superfamily II DNA and RNA helicases
44	1::GOAT_ENSP00000262193	101	27.4	5	5	1.381	PSMB1	Proteasome subunit beta type-1	20S proteasome, alpha and beta subunits
45	1::GOAT_ENSBTAP00000013079	234	22.7	5	5	1.425	RPS3A	40S ribosomal protein S3a	Ribosomal protein S3AE

Table 2 (continued)

Group ID	Accession no	Score	%Cov (95%)	Peptide (95%)	Unique peptide	vorfM_116: CK_119	Protein abbreviation	Protein description	COG function description
46	1::GOAT_ENSP00000378669	382	40.9	11	11	1.216	ALDOA	Fructose-bisphosphate aldolase A	Fructose-1,6-bisphosphate aldolase
47	1::GOAT_ENSP00000307288	65	11	6	6	1.245	MCM7	DNA replication licensing factor MCM7	Predicted ATPase involved in replication control, Cdc46/Mcm family
48	1::GOAT_ENSP00000357876	69	10.3	3	3	1.404	PSMD4	26S proteasome non-ATPase regulatory subunit 4	26S proteasome regulatory complex, subunit RPN10/PSMD4
49	1::GOAT_ENSBTAP00000001351	90	6.7	2	2	1.413	GDF10	Bone morphogenetic protein 3B	-
50	1::GOAT_ENSP00000262584	162	14	2	2	1.511	RPL8	60S ribosomal protein L8	Ribosomal protein L2
51	1::GOAT_ENSP00000359910	134	31.5	5	5	1.265	PSMA7	Proteasome subunit alpha type-7	20S proteasome, alpha and beta subunits
52	1::GOAT_ENSBTAP00000019980	23	4.6	1	1	1.675	CG059	UPF0539 protein C7orf59 homolog	-
53	1::goat_GLEAN_10016260	255	25.7	3	1	1.255	FTL	Ferritin light chain (Fragment)	Ferritin-like protein
54	1::GOAT_ENSP00000324111-D9	45	2.3	1	1	1.46	OR10AG1	Olfactory receptor 10AG1	-
55	1::GOAT_ENSP00000377385	61	1.8	1	1	1.34	Ppan	Suppressor of SWI4 1 homolog	-
56	1::GOAT_ENSBTAP00000018566	1208	17.9	8	8	1.666	CALD1	Caldesmon	-
57	1::GOAT_ENSBTAP00000000240	107	16.9	2	2	1.205	ATP6V1G1	V-type proton ATPase subunit G 1	-
58	1::GOAT_ENSP00000376290	232	24.7	5	5	1.695	TRA2B	Transformer-2 protein homolog beta	RNA-binding proteins (RRM domain)
59	1::GOAT_ENSP00000407602	300	8.4	13	13	1.511	MAP4	Microtubule-associated protein 4	-
60	1::GOAT_ENSBTAP00000053740	364	9.7	8	8	1.379	RRBP1	Ribosome-binding protein 1	PPE-repeat proteins
61	1::GOAT_ENSP00000328773	46	6.6	2	2	1.415	HEXIM1	Protein HEXIM1	-
62	1::GOAT_ENSBTAP00000043789	80	8.9	2	2	1.454	APOD	Apolipoprotein D	Bacterial lipocalin
63	1::goat_GLEAN_10013438	162	13.2	6	6	1.325	HNRNPU	Heterogeneous nuclear ribonucleoprotein U	-
64	1::GOAT_ENSBTAP00000015619	41	10.3	2	2	1.289	MRPL14	39S ribosomal protein L14, mitochondrial	Ribosomal protein L14
65	1::GOAT_ENSP00000415615	49	8.1	2	2	1.332	Csnk2b	Casein kinase II subunit beta	Casein kinase II, beta subunit
66	1::GOAT_ENSP00000315309	71	20.5	4	4	1.571	PSMA1	Proteasome subunit alpha type-1	20S proteasome, alpha and beta subunits
67	1::GOAT_ENSBTAP00000022763	293	13.3	7	7	1.359	ALB	Serum albumin	-
68	1::GOAT_ENSP00000281537	47	2.7	4	4	1.357	TJP1	Tight junction protein ZO-1	-

Table 2 (continued)

Group ID	Accession no	Score	%Cov (95%)	Peptide (95%)	Unique peptide	vorfM_116: CK_119	Protein abbreviation	Protein description	COG function description
69	1::GOAT_ENSBTAP00000013796	125	14.4	5	5	1.42	PA2G4	Proliferation-associated protein 2G4	Methionine aminopeptidase
70	1::GOAT_ENSBTAP00000013522	56	8.6	2	2	1.234	DHRS1	Dehydrogenase/reductase SDR family member 1	Dehydrogenases with different specificities (related to short-chain alcohol dehydrogenases)
71	1::GOAT_ENSBTAP00000011762	75	20.8	2	2	1.228	PFDN5	Prefoldin subunit 5	Predicted prefoldin, molecular chaperone implicated in de novo protein folding
72	1::goat_GLEAN_10013034	1401	24.9	5	3	1.45	NPM1	Nucleophosmin	-
73	1::GOAT_ENSP00000422319	229	13.8	11	11	1.235	MATR3	Matrin-3	-
74	1::GOAT_ENSP00000380362	83	4	2	2	1.455	EIF3D	Eukaryotic translation initiation factor 3 subunit D	-
75	1::GOAT_ENSP00000367806	102	7.5	1	1	1.283	Rps16	40S ribosomal protein S16	Ribosomal protein S9
76	1::GOAT_ENSP00000357206	1438	27.6	25	25	1.307	TANA	Tanabin	-
77	1::GOAT_ENSP00000301785	217	12.7	6	6	1.207	HNRNPUL2	Heterogeneous nuclear ribonucleoprotein U-like protein 2	-
78	1::GOAT_ENSBTAP00000016560	192	12	8	8	1.261	CDCP1	CUB domain-containing protein 1	-
79	1::GOAT_ENSBTAP00000026323	44	14.9	2	2	1.488	PRKCDBP	Protein kinase C delta-binding protein	-
80	1::GOAT_ENSP00000379888	285	42.5	7	7	1.564	Rps8	40S ribosomal protein S8	Ribosomal protein S8E
81	1::GOAT_ENSP00000381785	147	20.1	7	7	1.239	HSDL2	Hydroxysteroid dehydrogenase-like protein 2	Dehydrogenases with different specificities (related to short-chain alcohol dehydrogenases)
82	1::GOAT_ENSBTAP00000028994	37	9.3	3	3	1.303	DNAJB4	DnaJ homolog subfamily B member 4	DnaJ-class molecular chaperone
83	1::GOAT_ENSBTAP00000021229	51	4.1	1	1	1.225	SCN2B	Sodium channel subunit beta-2	-
84	1::GOAT_ENSBTAP00000017837	111	5.3	4	4	1.363	RBM12B	RNA-binding protein 12B	-
85	1::GOAT_ENSBTAP00000008609	46	12.4	2	2	1.591	HDGF	Hepatoma-derived growth factor OS = Bos taurus GN = HDGF PE = 2 SV = 1	-
86	1::GOAT_ENSBTAP00000004635	67	6.3	3	3	1.455	HPX	Hemopexin	-
87	1::GOAT_ENSP00000350990	104	2.9	3	3	1.274	TNKS1BP1	182 kDa tankyrase-1-binding protein	-
88	1::GOAT_ENSBTAP00000007584	27	0.5	1	1	2.199	NPHP3	Nephrocystin-3	FOG: TPR repeat
89	1::GOAT_ENSP00000309415	69	12	2	2	1.414	CLTB	Clathrin light chain B	-

Table 2 (continued)

Group ID	Accession no	Score	%Cov (95%)	Peptide (95%)	Unique peptide	vorfM_116: CK_119	Protein abbreviation	Protein description	COG function description
90	1::GOAT_ENSP00000361777	136	16.8	4	4	1.376	SET	Protein SET	-
91	1::GOAT_ENSP00000401336	515	30.6	9	9	1.348	Srsf1	Serine/arginine-rich splicing factor 1	RNA-binding proteins (RRM domain)
92	1::GOAT_ENSP00000370739	682	22.3	6	1	1.632	ENO3	Beta-enolase	Enolase
93	1::GOAT_ENSP00000353878	31	11.5	2	2	1.216	BAK1	Bcl-2 homologous antagonist/killer	-
94	1::GOAT_ENSBTAP00000012939	109	50	3	3	1.322	CXCL6	C-X-C motif chemokine 6	-
95	1::GOAT_ENSBTAP00000019232	208	18.2	5	5	1.397	SERPINE1	Plasminogen activator inhibitor 1	Serine protease inhibitor
96	1::GOAT_ENSBTAP00000041265	206	16.6	5	5	1.211	NDUFV3	NADH dehydrogenase [ubiquinone] flavoprotein 3, mitochondrial	-
97	1::GOAT_ENSBTAP00000029400	52	3.2	3	3	1.258	SPECC1L	Cytospin-A	Ca2 + -binding actin-bundling protein fimbrin/plastin (EF-Hand superfamily)
98	1::GOAT_ENSP00000362744	353	28.6	6	6	1.229	RPS4X	40S ribosomal protein S4, X isoform	Ribosomal protein S4E
99	1::GOAT_ENSP00000355011	210	21.1	5	5	1.272	ILF2	Interleukin enhancer-binding factor 2	-
100	1::GOAT_ENSP00000296674	67	15.5	2	2	1.38	Rps23	40S ribosomal protein S23	Ribosomal protein S12
101	1::GOAT_ENSBTAP00000053088	71	6.2	1	1	1.293	H1FX	Histone H1x OS = Homo sapiens	-
102	1::GOAT_ENSBTAP00000007571	96	6.4	3	3	1.36	FUS	RNA-binding protein FUS	-
103	1::goat_GLEAN_10000207	721	48.1	5	3	1.342	Tpm3	Tropomyosin alpha-3 chain	-
104	1::GOAT_ENSBTAP00000019184	94	29.3	3	3	1.232	RPL22	60S ribosomal protein L22	-
105	1::GOAT_ENSBTAP00000051168	327	9.6	4	2	1.497	HSPA6	Heat shock 70 kDa protein 6	Molecular chaperone
106	1::GOAT_ENSBTAP00000053339	133	9.2	9	9	1.325	ERC1	ELKS/Rab6-interacting/CAST family member 1	-
107	1::GOAT_ENSBTAP00000051256-D3	151	14.6	3	3	1.6	HIST1H1C	Histone H1.2	-
108	1::GOAT_ENSBTAP00000012735	182	19.6	3	2	1.46	YBX1	Nuclease-sensitive element-binding protein 1	Cold shock proteins
109	1::GOAT_ENSBTAP00000012544	283	37.4	9	9	1.519	RPS2	40S ribosomal protein S2	Ribosomal protein S5
110	1::GOAT_ENSP00000349428	212	11	4	3	1.222	PTBP1	Polypyrimidine tract-binding protein 1	-

Table 2 (continued)

Group ID	Accession no	Score	%Cov (95%)	Peptide (95%)	Unique peptide	vorfM_116: CK_119	Protein abbreviation	Protein description	COG function description
111	1::GOAT_ENSBTAP00000011484	300	19.5	6	6	1.485	SSB	Lupus La protein homolog	La protein, small RNA-binding pol III transcript stabilizing protein and related La-motif-containing proteins involved in translation
112	1::GOAT_ENSBTAP00000053296	129	4.3	3	3	1.418	PALM2	Paralemmin-2	-
113	1::GOAT_ENSBTAP00000020452	286	19.7	3	3	1.273	RPL18	60S ribosomal protein L18	Ribosomal protein L18E
114	1::GOAT_ENSBTAP00000049167	47	1.9	1	1	1.352	SUCNR1	Succinate receptor 1	-
115	1::GOAT_ENSBTAP00000049804	100	8.4	2	2	1.616	NUCKS1	Nuclear ubiquitous casein and cyclin-dependent kinase substrate 1	-
116	1::goat_GLEAN_10006421	106	7	2	2	1.525	DYNC1I2	Cytoplasmic dynein 1 intermediate chain 2	-
117	1::GOAT_ENSP00000415769	186	6.1	5	5	1.368	ITIH3	Inter-alpha-trypsin inhibitor heavy chain H3	Uncharacterized protein containing a von Willebrand factor type A (vWA) domain
118	1::GOAT_ENSP00000359506	154	8.8	4	3	1.509	FMR1	Fragile X mental retardation protein 1	-
119	1::GOAT_ENSBTAP00000042575	28	0.7	1	1	1.349	PPP4R4	Serine/threonine-protein phosphatase 4 regulatory subunit 4	-
120	1::GOAT_ENSP00000359345	133	25	7	7	1.535	RPL5	60S ribosomal protein L5	Ribosomal protein L18
121	1::GOAT_ENSP00000340278	249	38.6	5	5	1.292	PARK7	Protein DJ-1	Putative intracellular protease/amidase
122	1::GOAT_ENSBTAP00000019203	55	6.9	2	2	1.334	PSMA4	Proteasome subunit alpha type-4	20S proteasome, alpha and beta subunits
123	1::GOAT_ENSP00000353224	776	27.8	18	18	1.262	TFRC	Transferrin receptor protein 1	-
124	1::GOAT_ENSBTAP00000040563	32	3.8	2	2	1.218	SLC2A1	Solute carrier family 2, facilitated glucose transporter member 1	Permeases of the major facilitator superfamily
125	1::GOAT_ENSP00000376159	89	4.5	3	2	2.17	BCLAF1	Bcl-2-associated transcription factor 1	-
126	1::GOAT_ENSP00000379733	155	38.8	9	6	1.512	RPL7	60S ribosomal protein L7	Ribosomal protein L30/L7E
127	1::GOAT_ENSP00000362110	174	15.6	6	6	1.27	SF3A3	Splicing factor 3A subunit 3	Splicing factor 3a, subunit 3
128	1::GOAT_ENSBTAP00000002349	137	28.4	2	2	1.235	RPL36	60S ribosomal protein L36	Ribosomal protein L36E
129	1::goat_GLEAN_10017787	518	16.4	10	6	1.206	EZR	Ezrin	-
130	1::GOAT_ENSP00000378720	262	7.5	8	8	1.239	KTN1	Kinectin	-
131	1::GOAT_ENSP00000365950	111	8.1	1	1	1.656	RBM3	Putative RNA-binding protein 3	RNA-binding proteins (RRM domain)

Table 2 (continued)

Group ID	Accession no	Score	%Cov (95%)	Peptide (95%)	Unique peptide	vorfM_116: CK_119	Protein abbreviation	Protein description	COG function description
132	1::GOAT_ENSP00000354314	31	1.7	1	1	1.38	HAO2	Hydroxyacid oxidase 2	L-lactate dehydrogenase (FMN-dependent) and related alpha-hydroxy acid dehydrogenases
133	1::GOAT_ENSP00000306099	42	4.5	2	2	1.534	FGB	Fibrinogen beta chain	-
134	1::GOAT_ENSBTAP00000003636	55	8.5	2	2	1.325	PSMA3	Proteasome subunit alpha type-3	20S proteasome, alpha and beta subunits
135	1::GOAT_ENSP00000229270	278	47.2	6	5	1.897	TPI1	Triosephosphate isomerase	Triosephosphate isomerase
136	1::GOAT_ENSBTAP00000019039	186	17.3	4	4	1.234	HNRNPH3	Heterogeneous nuclear ribonucleoprotein H3	-
137	1::GOAT_ENSBTAP00000036278	37	5.7	3	3	1.27	CNP	2′,3′-cyclic-nucleotide 3′-phosphodiesterase	-
138	1::GOAT_ENSBTAP00000025094	163	9.4	3	3	1.206	HARS	Histidine–tRNA ligase, cytoplasmic	Histidyl-tRNA synthetase
139	1::GOAT_ENSP00000316042	136	14.4	2	2	1.23	HNRNPA0	Heterogeneous nuclear ribonucleoprotein A0	RNA-binding proteins (RRM domain)
140	1::GOAT_ENSP00000393738-D2	49	1.2	1	1	1.564	GALNT13	Polypeptide N-acetylgalactosaminyltransferase 13	-
141	1::GOAT_ENSP00000340176	68	17.7	3	3	1.208	RBPMS	RNA-binding protein with multiple splicing	-
142	1::goat_GLEAN_10004749	243	17.5	6	4	1.328	KRT10	Keratin, type I cytoskeletal 10	-
143	1::GOAT_ENSP00000346634	159	6.2	5	4	1.551	THRAP3	Thyroid hormone receptor-associated protein 3	-
144	1::GOAT_ENSBTAP00000023664	90	32.7	3	3	1.307	ERH	Enhancer of rudimentary homolog (Fragment)	-
145	1::GOAT_ENSP00000349140	148	14.4	1	1	1.337	MTPN	Myotrophin	FOG: Ankyrin repeat
146	1::GOAT_ENSP00000405965	82	13.5	1	1	2.004	SUMO2	Small ubiquitin-related modifier 2	Ubiquitin-like protein (sentrin)
146	1::GOAT_ENSP00000409666	82	10.1	1	1				
147	1::GOAT_ENSBTAP00000001518	78	8.4	2	2	1.49	CLTA	Clathrin light chain A	-
148	1::GOAT_ENSP00000373930	91	11.2	8	8	1.344	KIAA1967	DBIRD complex subunit KIAA1967	-
149	1::GOAT_ENSBTAP00000050222	380	23.7	4	4	1.562	RPL17	60S ribosomal protein L17	Ribosomal protein L22
149	1::goat_GLEAN_10016995	380	23.9	4	4				
150	1::GOAT_ENSBTAP00000041518	56	1	1	1	1.589	Ky	Kyphoscoliosis peptidase	Uncharacterized protein involved in cytokinesis, contains TGc (transglutaminase/protease-like) domain

Table 2 (continued)

Group ID	Accession no	Score	%Cov (95%)	Peptide (95%)	Unique peptide	vorfM_116: CK_119	Protein abbreviation	Protein description	COG function description
151	1::GOAT_ENSBTAP00000016153	61	47.9	5	5	1.275	SNRPD2	Small nuclear ribonucleoprotein Sm D2	Small nuclear ribonucleoprotein (snRNP) homolog
152	1::GOAT_ENSP00000420195	102	16.7	4	4	1.259	Srsf10	Serine/arginine-rich splicing factor 10	-
153	1::GOAT_ENSBTAP00000004122	48	12.6	2	2	1.369	NDUFAF4	NADH dehydrogenase [ubiquinone] 1 alpha subcomplex assembly factor 4	-
154	1::GOAT_ENSP00000318195	675	22.8	15	13	1.499	NCL	Nucleolin	RNA-binding proteins (RRM domain)
155	1::goat_GLEAN_10000538	34	9.8	2	2	1.407	HVM63	Ig heavy chain Mem5 (Fragment)	-
156	1::GOAT_ENSBTAP00000047729-D2	217	20.5	7	6	1.382	LDHA	L-lactate dehydrogenase A chain	Malate/lactate dehydrogenases
157	1::GOAT_ENSP00000253814	50	7.5	2	2	1.578	NDFIP1	NEDD4 family-interacting protein 1	-
158	1::GOAT_ENSBTAP00000002326	699	85.2	7	7	1.386	RPLP2	60S acidic ribosomal protein P2 (Fragment)	Ribosomal protein L12E/L44/L45/RPP1/RPP2
159	1::GOAT_ENSBTAP00000008357	43	7.5	2	2	1.435	CTGF	Connective tissue growth factor	-
160	1::GOAT_ENSP00000364119	90	13.5	3	3	1.263	EIF2S2	Eukaryotic translation initiation factor 2 subunit 2	Translation initiation factor 2, beta subunit (eIF-2beta)/eIF-5 N-terminal domain
160	1::goat_GLEAN_10014323	90	13.5	3	3				
161	1::GOAT_ENSBTAP00000027001	32	0.4	1	1	1.477	PSME4	Proteasome activator complex subunit 4	-
162	1::GOAT_ENSBTAP00000017816	57	12.6	3	3	1.414	PSMB6	Proteasome subunit beta type-6	20S proteasome, alpha and beta subunits
163	1::GOAT_ENSP00000338727	93	1.9	1	1	1.279	Lrrfip2	Leucine-rich repeat flightless-interacting protein 2	-
164	1::GOAT_ENSBTAP00000011029	93	7.7	4	4	1.553	CAST	Calpastatin	-
165	1::GOAT_ENSBTAP00000017988	158	10.4	5	5	1.531	PGD	6-phosphogluconate dehydrogenase, decarboxylating	6-phosphogluconate dehydrogenase
166	1::GOAT_ENSP00000376055	195	38.7	5	5	1.226	EEF1B	Elongation factor 1-beta	Translation elongation factor EF-1beta
167	1::GOAT_ENSBTAP00000029284	117	30.7	4	4	1.723	SUB1	Activated RNA polymerase II transcriptional coactivator p15	-
168	1::GOAT_ENSP00000377469	158	26.1	4	4	1.247	NACA	Nascent polypeptide-associated complex subunit alpha	Transcription factor homologous to NACalpha-BTF3

Table 2 (continued)

Group ID	Accession no	Score	%Cov (95%)	Peptide (95%)	Unique peptide	vorfM_116: CK_119	Protein abbreviation	Protein description	COG function description
169	1::GOAT_ENSBTAP00000015875-D2	108	24.2	4	4	1.596	RPS19	40S ribosomal protein S19	Ribosomal protein S19E (S16A)
170	1::GOAT_ENSP00000403265	1786	41.3	21	21	1.606	PKM2	Pyruvate kinase isozymes M1/M2	Pyruvate kinase
171	1::GOAT_ENSBTAP00000028486	68	24.3	5	3	1.755	ANP32B	Acidic leucine-rich nuclear phosphoprotein 32 family member B	-
172	1::GOAT_ENSBTAP00000003340	86	23	5	4	1.221	Fbl	rRNA 2′-O-methyltransferase fibrillarin	Fibrillarin-like rRNA methylase
173	1::GOAT_ENSBTAP00000001791-D2	96	18.1	2	2	1.252	RPS12	40S ribosomal protein S12	Ribosomal protein HS6-type (S12/L30/L7a)
173	1::goat_GLEAN_10019219	96	18.7	2	2				
174	1::GOAT_ENSBTAP00000009803	137	23.5	3	3	1.21	RPL10	60S ribosomal protein L10	Ribosomal protein L16/L10E
175	1::goat_GLEAN_10019253	401	32.8	5	2	1.541	PPIA	Peptidyl-prolyl cis–trans isomerase A	Peptidyl-prolyl cis–trans isomerase (rotamase)—cyclophilin family
176	1::GOAT_ENSBTAP00000031070	73	11	4	4	1.215	CNDP2	Cytosolic non-specific dipeptidase	Acetylornithine deacetylase/Succinyl-diaminopimelate desuccinylase and related deacylases
177	1::GOAT_ENSBTAP00000013650	92	12.1	2	2	1.866	TALDO1	Transaldolase (Fragment)	Transaldolase
178	1::GOAT_ENSBTAP00000025691	144	6.9	2	2	1.247	MDH1	Malate dehydrogenase, cytoplasmic	Malate/lactate dehydrogenases
179	1::GOAT_ENSP00000408907-D2	427	26.2	9	3	1.231	HSPA1B	Heat shock 70 kDa protein 1B	Molecular chaperone
180	1::GOAT_ENSBTAP00000014585	71	8.9	1	1	1.518	TTR	Transthyretin	Transthyretin-like protein
181	1::GOAT_ENSBTAP00000006383	468	52.2	11	11	1.414	PRDX6	Peroxiredoxin-6 (Fragments)	Peroxiredoxin
182	1::GOAT_ENSP00000381916	557	10.1	6	6	1.307	EIF3C	Eukaryotic translation initiation factor 3 subunit C	-
183	1::GOAT_ENSBTAP00000001309	129	19.7	3	3	1.291	PSMA2	Proteasome subunit alpha type-2	20S proteasome, alpha and beta subunits
183	1::goat_GLEAN_10020553	129	20.1	3	3				
184	1::GOAT_ENSBTAP00000037502	104	1.6	3	3	1.345	IGF2R	Cation-independent mannose-6-phosphate receptor	-
185	1::GOAT_ENSP00000369421	21	1.1	1	1	2.041	FUT10	Alpha-(1,3)-fucosyltransferase 10	-
186	1::GOAT_ENSBTAP00000053565	339	11.1	8	8	1.298	ILF3	Interleukin enhancer-binding factor 3	-
187	1::GOAT_ENSBTAP00000002642	232	13.7	3	3	1.273	RPL14	60S ribosomal protein L14	Ribosomal protein L14E/L6E/L27E

Table 2 (continued)

Group ID	Accession no	Score	%Cov (95%)	Peptide (95%)	Unique peptide	vorfM_116: CK_119	Protein abbreviation	Protein description	COG function description
188	1::GOAT_ENSP00000389536	102	11.4	7	5	1.328	FUBP1	Far upstream element-binding protein 1	-
189	1::GOAT_ENSBTAP00000020701	148	24.3	5	5	1.271	HMOX1	Heme oxygenase 1	Heme oxygenase
190	1::GOAT_ENSP00000354884	35	1.9	1	1	1.539	RASSF9	Ras association domain-containing protein 9	-
191	1::GOAT_ENSP00000317786	138	4	4	4	1.298	MPRIP	Myosin phosphatase Rho-interacting protein	-
192	1::GOAT_ENSBTAP00000019001	87	3.8	2	2	1.311	TOMM70A	Mitochondrial import receptor subunit TOM70	FOG: TPR repeat
193	1::GOAT_ENSBTAP00000022382	53	15	2	2	1.437	PFDN6	Prefoldin subunit 6	Prefoldin, chaperonin cofactor
194	1::GOAT_ENSBTAP00000023197	46	7.6	4	4	1.348	ADAM9	Disintegrin and metalloproteinase domain-containing protein 9	-
195	1::GOAT_ENSP00000362352	64	11.3	3	2	1.204	H2AFY2	Core histone macro-H2A.2	Histone H2A
196	1::GOAT_ENSBTAP00000021658	115	6	3	3	1.431	PREP	Prolyl endopeptidase	Serine proteases of the peptidase family S9A
197	1::GOAT_ENSP00000215909	750	62.3	6	6	1.507	LGALS1	Galectin-1	-
198	1::GOAT_ENSP00000378172	149	5.2	2	2	1.422	ZNF207	Zinc finger protein 207	-
199	1::GOAT_ENSBTAP00000025659	40	6.2	3	3	1.29	NARS	Asparagine–tRNA ligase, cytoplasmic	Aspartyl/asparaginyl-tRNA synthetases
200	1::GOAT_ENSP00000346022	160	18.8	3	3	1.441	RPL9	60S ribosomal protein L9	Ribosomal protein L6P/L9E
201	1::GOAT_ENSP00000322016	121	14	6	6	1.297	PUF60	Poly(U)-binding-splicing factor PUF60	RNA-binding proteins (RRM domain)
202	1::GOAT_ENSBTAP00000003532	92	2.1	1	1	1.49	RNGTT	mRNA-capping enzyme	mRNA capping enzyme, guanylyltransferase (alpha) subunit
203	1::GOAT_ENSP00000363676	218	16.9	3	3	1.379	RPL11	60S ribosomal protein L11	Ribosomal protein L5
204	1::GOAT_ENSP00000369317-D4	302	11.3	5	3	1.663	KRT1	Keratin, type II cytoskeletal 1	-
205	1::GOAT_ENSBTAP00000008363	21	10.7	1	1	1.844	NHP2	H/ACA ribonucleoprotein complex subunit 2	Ribosomal protein HS6-type (S12/L30/L7a)
206	1::GOAT_ENSBTAP00000001113	239	9.1	7	7	1.202	PARP1	Poly [ADP-ribose] polymerase 1	-
207	1::GOAT_ENSP00000265753	149	18.1	3	3	1.249	EIF4H	Eukaryotic translation initiation factor 4H	RNA-binding proteins (RRM domain)
208	1::GOAT_ENSP00000338095	513	16.6	5	5	1.211	HNRNPC	Heterogeneous nuclear ribonucleoprotein C	-
209	1::GOAT_ENSP00000368927	65	18	2	2	1.369	Eif1ax	Eukaryotic translation initiation factor 1A, X-chromosomal	Translation initiation factor 1 (IF-1)

Table 2 (continued)

Group ID	Accession no	Score	%Cov (95%)	Peptide (95%)	Unique peptide	vorfM_116: CK_119	Protein abbreviation	Protein description	COG function description
210	1::GOAT_ENSP00000358939	119	13.4	6	6	1.266	SARS	Serine–tRNA ligase, cytoplasmic	Seryl-tRNA synthetase
211	1::GOAT_ENSP00000404545	76	6.6	4	4	1.502	Safb	Scaffold attachment factor B1	-
212	1::GOAT_ENSBTAP00000041837	130	10.4	3	3	1.243	Raly	RNA-binding protein Raly	-
213	1::GOAT_ENSBTAP00000027348	126	16.9	6	5	1.296	IDH1	Isocitrate dehydrogenase [NADP] cytoplasmic	Isocitrate dehydrogenases
214	1::GOAT_ENSBTAP00000018888	30	6.9	1	1	1.917	RPL35A	60S ribosomal protein L35a	Ribosomal protein L35AE/L33A
215	1::GOAT_ENSBTAP00000009564	334	13.6	10	10	1.368	TF	Serotransferrin	-
216	1::GOAT_ENSBTAP00000020564	77	5.3	2	2	1.312	SRSF11	Serine/arginine-rich splicing factor 11	-
217	1::GOAT_ENSBTAP00000052105	213	31.5	4	4	1.437	Rps13	40S ribosomal protein S13	Ribosomal protein S15P/S13E
218	1::GOAT_ENSBTAP00000031700	45	13.3	2	2	1.546	RPL28	60S ribosomal protein L28	-
219	1::GOAT_ENSBTAP00000040484	1295	33.1	9	9	1.677	GAPDH	Glyceraldehyde-3-phosphate dehydrogenase (Fragment)	Glyceraldehyde-3-phosphate dehydrogenase/erythrose-4-phosphate dehydrogenase
220	1::GOAT_ENSBTAP00000037041	99	19.9	3	3	1.405	Rpl23a	60S ribosomal protein L23a	Ribosomal protein L23
221	1::GOAT_ENSBTAP00000025484	74	18.3	2	2	1.34	RPS20	40S ribosomal protein S20	Ribosomal protein S10
222	1::GOAT_ENSBTAP00000023484	111	14.9	2	2	2.097	CDV3	Protein CDV3 homolog	-

Table 3 Downregulated proteins identified by iTRAQ analysis of ORFV-infected GSF cells. These proteins had expression ratios < 0.8 relative to the control group at the same time postinfection

Group ID	Accession no	Score	Cov (95%)	Peptide (95%)	Unique peptide	vorfM_116: CK_119	Protein abbreviation	Protein description	COG function description
1	1::GOAT_ENSP00000385942	173	7.2	6	6	0.784	Xpo1	Exportin-1	Importin beta-related nuclear transport receptor
2	1::GOAT_ENSP00000362335	203	30.8	5	3	0.824	SAR1A	GTP-binding protein SAR1a	GTPase SAR1 and related small G proteins
3	1::GOAT_ENSP00000304408	833	14.4	13	12	0.566	COL3A1	Collagen alpha-1(III) chain	-
4	1::GOAT_ENSBTAP00000007515	451	51.1	6	6	0.732	CRABP2	Cellular retinoic acid-binding protein 2	-
5	1::GOAT_ENSP00000414942	72	5.1	1	1	0.688	IST1	IST1 homolog	-
6	1::GOAT_ENSBTAP00000014801	125	14.6	1	1	0.775	NDUFA4	NADH dehydrogenase [ubiquinone] 1 alpha subcomplex subunit 4	-
7	1::GOAT_ENSP00000357980	386	39	9	9	0.745	HTRA1	Serine protease HTRA1	Trypsin-like serine proteases, typically periplasmic, contain C-terminal PDZ domain
8	1::GOAT_ENSP00000216479	96	17	4	4	0.805	AHSA1	Activator of 90 kDa heat shock protein ATPase homolog 1	Activator of HSP90 ATPase
9	1::GOAT_ENSP00000360939	66	6.2	1	1	0.808	CMPK1	UMP-CMP kinase	Adenylate kinase and related kinases
10	1::GOAT_ENSP00000262288	199	18.8	4	4	0.8	SCPEP1	Retinoid-inducible serine carboxypeptidase	Carboxypeptidase C (cathepsin A)
11	1::GOAT_ENSBTAP00000031937	111	17.3	4	4	0.812	Ech1	Delta(3,5)-Delta(2,4)-dienoyl-CoA isomerase, mitochondrial	Enoyl-CoA hydratase/carnitine racemase
12	1::GOAT_ENSBTAP00000017298	167	2.6	2	2	0.739	PLAA	Phospholipase A-2-activating protein	FOG: WD40 repeat
13	1::goat_GLEAN_10009864	87	8.5	2	2	0.704	TWF2	Twinfilin-2	-
14	1::GOAT_ENSP00000381607	87	11.9	1	1	0.72	GSTP1	Glutathione S-transferase P	-
15	1::GOAT_ENSP00000361508	84	13.6	4	4	0.746	PLTP	Phospholipid transfer protein	-
16	1::GOAT_ENSBTAP00000045426	183	3.3	2	2	0.832	NAA15	N-alpha-acetyltransferase 15, NatA auxiliary subunit	FOG: TPR repeat
17	1::GOAT_ENSP00000269321	446	41.7	6	6	0.818	ARHGDIA	Rho GDP-dissociation inhibitor 1	-
18	1::GOAT_ENSP00000205061	106	7.5	6	6	0.754	Glg1	Golgi apparatus protein 1	-
19	1::GOAT_ENSP00000348775	91	6	3	3	0.816	ACOX3	Peroxisomal acyl-coenzyme A oxidase 3	Acyl-CoA dehydrogenases
20	1::GOAT_ENSBTAP00000003959	122	22.5	1	1	0.815	GNG2	Guanine nucleotide-binding protein G(I)/G(S)/G(O) subunit gamma-2	-
21	1::GOAT_ENSBTAP00000043782	102	15.1	2	2	0.813	CAV1	Caveolin-1	-
22	1::GOAT_ENSBTAP00000005837	56	3.7	2	2	0.778	Ipo9	Importin-9	CAS/CSE protein involved in chromosome segregation
23	1::GOAT_ENSBTAP00000010389	80	15.1	2	2	0.722	FIS1	Mitochondrial fission 1 protein	-
24	1::GOAT_ENSP00000416650	102	14.6	3	3	0.772	PSME2	Proteasome activator complex subunit 2	-
25	1::GOAT_ENSP00000360860	73	12.9	5	5	0.751	IFIT5	Interferon-induced protein with tetratricopeptide repeats 5	-

Table 3 (continued)

Group ID	Accession no	Score	Cov (95%)	Peptide (95%)	Unique peptide	vorfM_116: CK_119	Protein abbreviation	Protein description	COG function description
26	1::GOAT_ENSP00000407726	237	14.5	9	9	0.676	VWA5A	von Willebrand factor A domain-containing protein 5A	Uncharacterized protein containing a von Willebrand factor type A (vWA) domain
27	1::goat_GLEAN_10015090	107	22.2	2	2	0.812	ATP5J	ATP synthase-coupling factor 6, mitochondrial	-
28	1::GOAT_ENSP00000381803	116	18.8	5	4	0.816	MAPK1	Mitogen-activated protein kinase 1	Serine/threonine protein kinase
29	1::GOAT_ENSBTAP00000007028	133	16.9	3	3	0.71	ARPC3	Actin-related protein 2/3 complex subunit 3	-
30	1::GOAT_ENSP00000264933	106	23.2	3	3	0.789	Pdcd6	Programmed cell death protein 6	-
31	1::GOAT_ENSBTAP00000020484	209	8.1	8	8	0.8	TBCD	Tubulin-specific chaperone D	Beta-tubulin folding cofactor D
32	1::GOAT_ENSBTAP00000030311	135	20	3	3	0.706	SAA1	Serum amyloid A protein	-
33	1::GOAT_ENSP00000409204	211	13.3	7	7	0.805	SUN2	SUN domain-containing protein 2	-
34	1::GOAT_ENSBTAP00000036255	182	24.6	5	5	0.796	LEPREL4	Synaptonemal complex protein SC65	-
35	1::GOAT_ENSP00000252951-D2	180	14.8	2	2	0.777	HBA	Hemoglobin subunit alpha-1/2	-
36	1::GOAT_ENSBTAP00000005713	645	22.2	7	7	0.803	SERPINC1	Antithrombin-III	Serine protease inhibitor
37	1::GOAT_ENSP00000394338	73	7.1	2	2	0.779	PPP2R4	Serine/threonine-protein phosphatase 2A activator	Phosphotyrosyl phosphatase activator
38	1::GOAT_ENSP00000382533	151	14.8	4	3	0.761	NAP1L4	Nucleosome assembly protein 1-like 4	-
39	1::GOAT_ENSBTAP00000053644	2353	43.4	39	39	0.827	Vcl	Vinculin	-
40	1::GOAT_ENSBTAP00000024445-D2	338	34.5	11	11	0.744	SERPINB1	Leukocyte elastase inhibitor	Serine protease inhibitor
41	1::GOAT_ENSBTAP00000005181	72	3.1	1	1	0.823	UBP1	Upstream-binding protein 1	-
42	1::GOAT_ENSBTAP00000032864	412	45.3	7	2	0.755	PGAM1	Phosphoglycerate mutase 1	Phosphoglycerate mutase 1
43	1::GOAT_ENSBTAP00000024227	148	14.8	5	5	0.795	DAK	Bifunctional ATP-dependent dihydroxyacetone kinase/FAD-AMP lyase (cyclizing)	Dihydroxyacetone kinase
44	1::GOAT_ENSBTAP00000026449	449	15.9	7	7	0.825	PPP2R1A	Serine/threonine-protein phosphatase 2A 65 kDa regulatory subunit A alpha isoform	-
45	1::GOAT_ENSP00000407487	153	9.2	7	7	0.813	UNC45A	Protein unc-45 homolog A	FOG: TPR repeat
46	1::GOAT_ENSP00000425006	98	6.4	3	3	0.825	ACSL1	Long-chain-fatty-acid–CoA ligase 1	Long-chain acyl-CoA synthetases (AMP-forming)
47	1::GOAT_ENSP00000227322	65	10.5	4	4	0.826	ZNF259	Zinc finger protein ZPR1	C4-type Zn-finger protein
48	1::GOAT_ENSP00000334008	218	15.9	4	4	0.761	PARVA	Alpha-parvin	-
49	1::GOAT_ENSP00000351740	94	7.1	3	3	0.795	FAM114A1	Protein NOXP20	-
50	1::GOAT_ENSBTAP00000035984	104	5.8	4	4	0.806	DNM2	Dynamin-2	Predicted GTPases (dynamin-related)

Table 3 (continued)

Group ID	Accession no	Score	Cov (95%)	Peptide (95%)	Unique peptide	vorfM_116: CK_119	Protein abbreviation	Protein description	COG function description
51	1::GOAT_ENSP00000369059	57	3.2	3	3	0.785	SEC24D	Protein transport protein Sec24D	Vesicle coat complex COPII, subunit SEC24/subunit SFB2/ subunit SFB3
52	1::GOAT_ENSBTAP00000011388	188	27.1	8	8	0.784	SULT1A1	Sulfotransferase 1A1	-
53	1::GOAT_ENSP00000340211	122	10.6	3	3	0.709	CORO1B	Coronin-1B	FOG: WD40 repeat
54	1::GOAT_ENSP00000395277	41	1.3	2	2	0.825	K0913	Zinc finger SWIM domain-containing protein KIAA0913	Uncharacterized conserved protein
55	1::GOAT_ENSBTAP00000051130	116	2.6	3	3	0.721	LAMB2	Laminin subunit beta-2	-
56	1::GOAT_ENSP00000229268	186	13.3	8	8	0.743	Usp5	Ubiquitin carboxyl-terminal hydrolase 5	Isopeptidase T
57	1::GOAT_ENSBTAP00000031243	1622	26	8	5	0.812	SERPINB2	Plasminogen activator inhibitor 2	Serine protease inhibitor
58	1::GOAT_ENSBTAP00000017069	162	23.1	9	9	0.824	Fam129b	Niban-like protein 1	-
59	1::GOAT_ENSBTAP00000033771	1409	27.9	25	25	0.702	COL1A2	Collagen alpha-2(I) chain	-
60	1::GOAT_ENSBTAP00000014960	45	9.8	3	3	0.819	ASAH1	Acid ceramidase	-

Fig. 3 Classification of the identified proteins based on their functional annotations using Gene Ontology enrichment analysis. (A) Cellular components of the identified proteins. (B) Molecular functions of the identified proteins. (C) Biological processes of the identified proteins. (D) Gene Ontology enrichment analysis of cellular components of differentially expressed proteins. (E) Gene Ontology enrichment analysis of molecular functions of differentially expressed proteins. (F) Gene Ontology enrichment analysis of biological processes of differentially expressed proteins. (G) COG classification of differentially expressed proteins. *P*-values were calculated using MetaCore in the GeneGO package (https://www.genego.com/)

information complementary to the protein expression data obtained by proteomics analysis.

The subcellular localization of HSPA1B

GSF cells were transfected with the recombinant plasmid pEGFP-HSPA1B for transient expression. The pEGFP-HSPA1B protein was used to observe the subcellular localization of HSPA1B using CLSM (Fig. 5A). Following DAPI staining, the nuclear excitation of the blue fluorescence was monitored (Fig. 5B) while the subcellular localization of pEGFP-N1 was monitored (Fig. 5D and E). Compared with pEGFP-N1 (Fig. 5F), the overlap of fluorescence in Fig. 5A and B indicated that the HSPA1B protein was mainly distributed in the cytoplasm of GSF cells (Fig. 5C).

Inhibition of ORFV proliferation by HSPA1B

GSF cells were transfected with pEGFP-HSPA1B, cultured for 18 h, and infected with ORFV. Cell suspension samples were collected at different time points after infection to measure virus proliferation by RT-qPCR. The results indicated that the difference in viral proliferation at 6 and 15 h postinfection between HSPA1B overexpressing cells and the control cells was not statistically significant. However, at 24 and 36 h postinfection, the viral genome copy number was considerably lower in cells overexpressing HSPA1B, indicating that this protein inhibits proliferation of ORFV in GSF cells (Fig. 6A). Next, we examined ORFV replication in HSPA1B-downregulated cells. HSPA1B was knocked down in GSF cells using RNAi. Three HSPA1B small interfering RNAs (siRNAs) were designed and synthesized, and their silencing efficiency was evaluated using a Western blot assay. SiRNA-517 was found to be the most efficient for decreasing HSPA1B expression (Fig. 6B). GSF cells were transfected with negative- control (NC) siRNA or siRNA-517 and then infected with equal amounts of ORFV. The siRNA knockdown efficiency was confirmed by Western blotting, and the levels of viral RNA and viral proteins in the siRNA-517 cells were compared to NC siRNA cells at different time points after virus infection. The levels of ORFV replication were higher in HSPA1B siRNA cells than

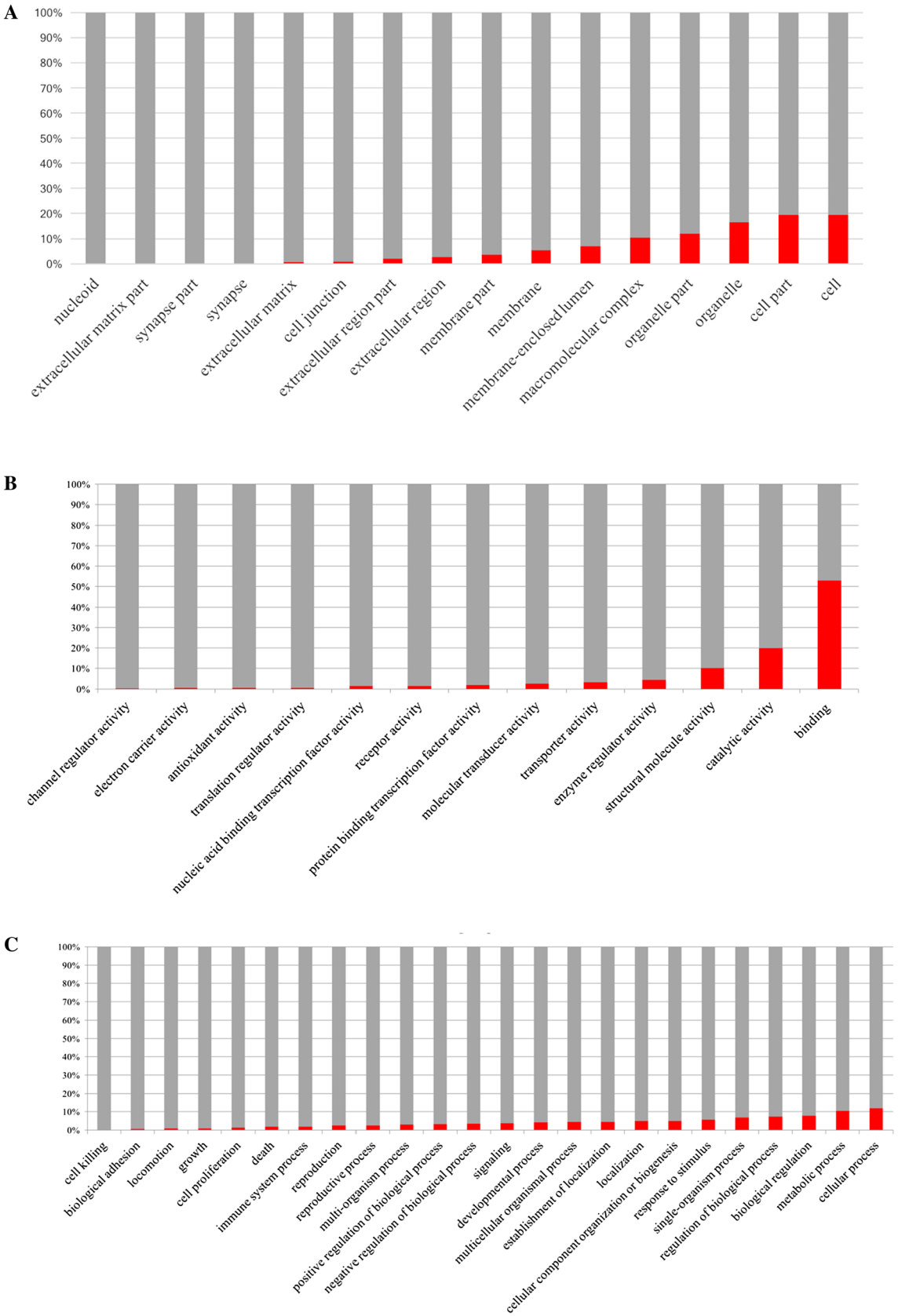
A
100%
90%
80%
70%
60%
50%
40%
30%
20%
10%
0%
nucleoid
extracellular matrix part
synapse part
synapse
extracellular matrix
cell junction
extracellular region part
extracellular region
membrane part
membrane
membrane-enclosed lumen
macromolecular complex
organelle part
organelle
cell part
cell
B
channel regulator activity
electron carrier activity
antioxidant activity
translation regulator activity
nucleic acid binding transcription factor activity
receptor activity
protein binding transcription factor activity
molecular transducer activity
transporter activity
enzyme regulator activity
structural molecule activity
catalytic activity
binding
C
cell killing
biological adhesion
locomotion
growth
cell proliferation
death
immune system process
reproduction
reproductive process
multi-organism process
positive regulation of biological process
negative regulation of biological process
signaling
developmental process
multicellular organismal process
establishment of localization
localization
cellular component organization or biogenesis
response to stimulus
single-organism process
regulation of biological process
biological regulation
metabolic process
cellular process

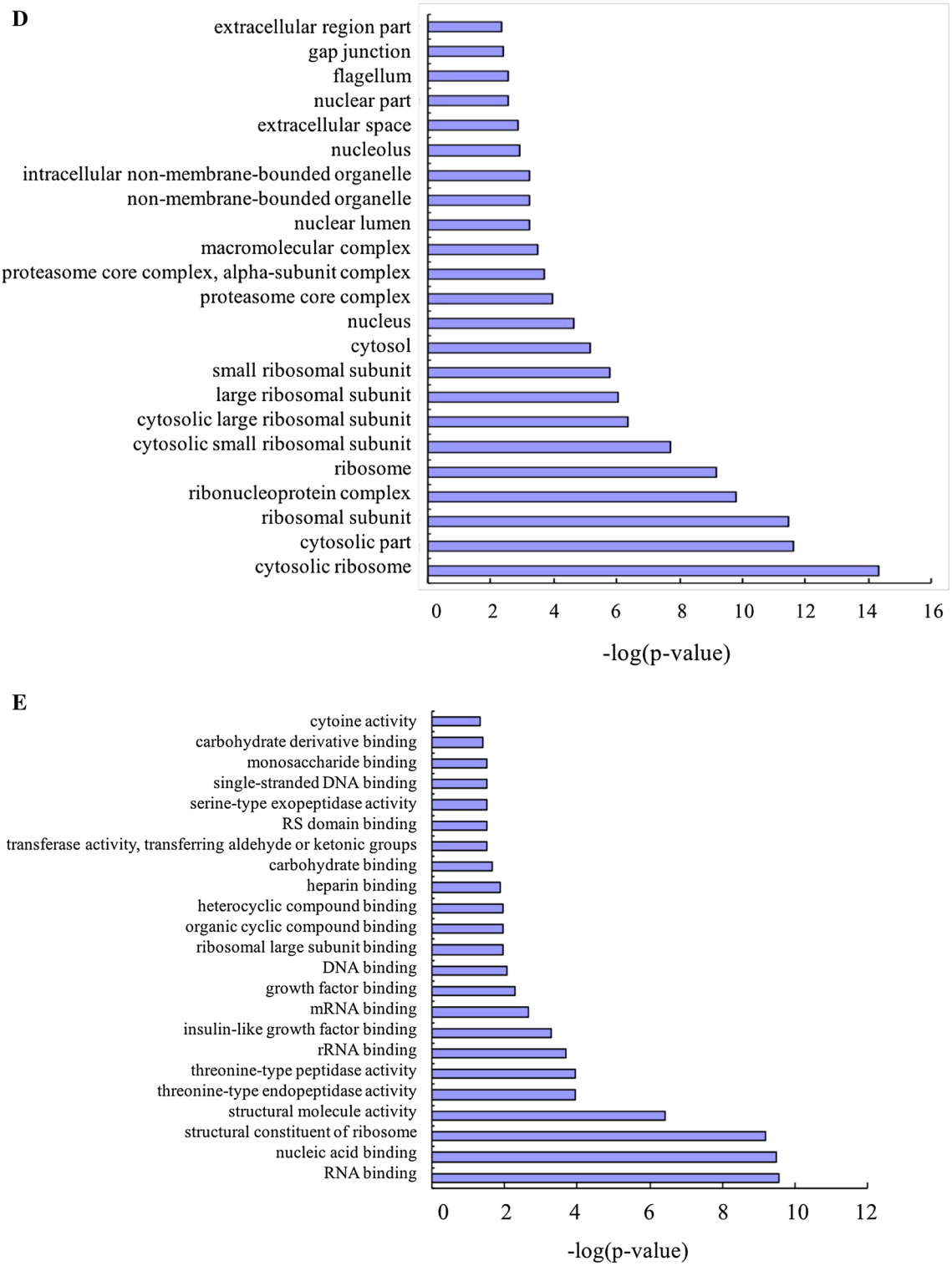

Fig. 3 (continued)

in control cells (Fig. 6C-E), suggesting that ORFV replication was significantly enhanced in the HSPA1B knockdown cells. These data suggest that HSPA1B has an inhibitory effect on ORFV replication in GSF cells.

Discussion

ORFV is an epitheliotropic virus that infects damaged or scarified skin and replicates in regenerating epidermal

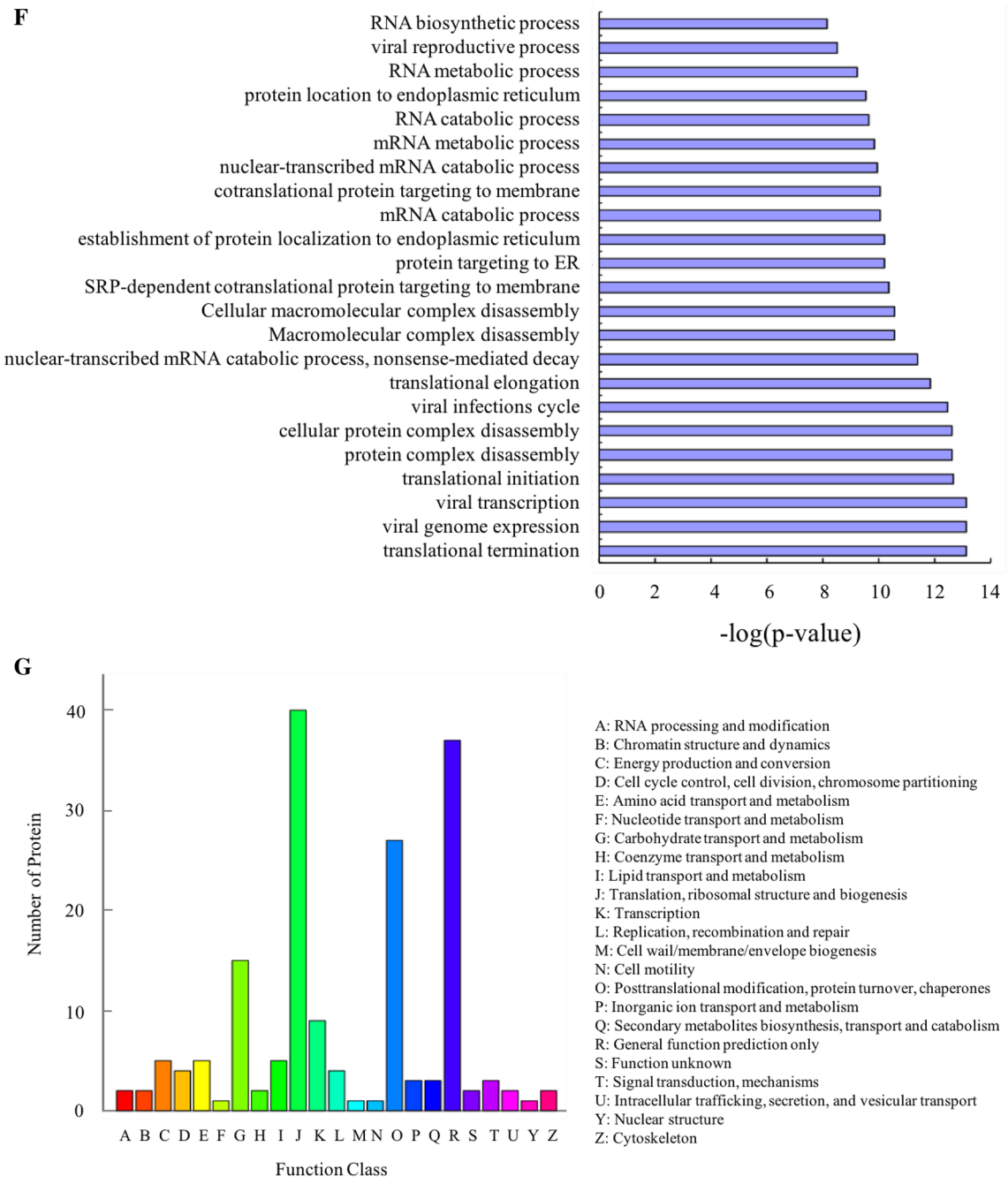

Fig. 3 (continued)

keratinocytes [27]. In a previous study, healthy OFTu cells were inoculated with a filtered viral suspension, and CPE was observed after 7–9 days. After five blind passages of ORFV, approximately 80% of the cells exhibited rounding, detachment, and clustering, creating a net-like form [9]. In the present study, the proliferation of GSF cells infected with ORFV was studied for the first time, using virus titration, microscopic observations, and RT-qPCR. The data indicated that GSF cells are susceptible to ORFV infection. The proliferation rate was initially slow but increased from 12 to 72 h postinfection. A one-step growth curve of ORFV in GSF cells showed that the intracellular viral level was the highest at 36 h postinfection. By 60 h, the cells had detached from the cell plate and the viral titer decreased, possibly due to the lysis of the infected cells. Since GSF cells are derived from the primary host of ORF, they provide a good model system for understanding the changes that occur in these cells following infection with ORFV. In the present

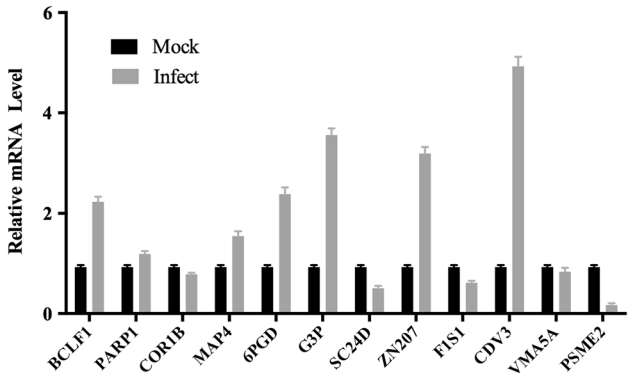

Fig. 4 Confirmation of differential expression by RT-qPCR. RT-qPCR was used to verify the differences in the transcription levels of differentially expressed proteins. The results indicated that the abundance of BCLF1, MAP4, 6PGD, G3P, ZN207, and CDV3 mRNA increased, whereas the expression levels of SC24D, FIS1, COR1B, and PSME2 decreased. The expression level of the PARP1 gene was upregulated, although the results were not conclusive. The mRNA level of VMA5A was upregulated following viral infection, but RT-qPCR and LC–MS/MS assays showed a decrease in the level of the corresponding protein. This inconsistency could be due to post-translational modification, including methylation, phosphorylation, or acetylation, or protein for unknown reasons

study, iTRAQ LC – MS/MS was applied for the first time to identify differentially expressed proteins in ORFV-infected GSF cells. The data demonstrated that 282 proteins were differentially expressed, 222 of which were upregulated and 60 of which were downregulated. Changes in mRNA levels measured by RT-qPCR were in agreement with the changes observed for the corresponding proteins by iTRAQ. These findings may be helpful for elucidating the molecular mechanisms by which target cells interact with the virus.

The host cytoskeletal network participates in the transport of viral components, particularly during the stages of entry and exit of the virus [30]. Viral components either hijack the cytoplasmic membrane traffic or interact directly with the cytoskeletal transport machinery [8]. In the present study, the expression levels of two specific proteins involved in cytoskeleton networks and cell communication were altered following ORFV infection. TBCD expression was downregulated, and SPECC1L expression was upregulated.

CD9 promotes adeno-associated virus type 2 infection of mammary carcinoma cells with low cell surface expression of heparan sulfate proteoglycans [19]. Parseval et al. [6] showed that the monoclonal antibody MAb vpg15, which targets a determinant of the feline cell surface marker CD9, which may serve as a receptor or co-receptor for feline immunodeficiency virus (FIV), markedly delayed infection with that virus. In the present study, CD9 was found to be upregulated in infected cells.

We also observed differential expression of components of several ubiquitin-mediated protein degradation pathways in ORFV-infected GSF cells. UBP5 is able to hydrolyze conjugates of the ubiquitin-like protein ISG15, as demonstrated in previous experiments in which these conjugates were shown to bind to the suicide probe ISG15-VS, which in turn inhibited protein degradation [36]. In the present study, UBP5 expression was downregulated, and PSMA7 expression was upregulated in ORFV-infected GSF cells. PSMA7 is a component of the 26S proteasome, participating in protein degradation and cell apoptosis. However, PMSA6 and PSME3, which belong to the same protein family, exhibited downregulated expression in infectious bursal disease virus (IBDV)-infected chicken embryo fibroblast (CEF) cells, suggesting that different viruses may use different pathways to regulate protein degradation and cell apoptosis [43].

It is noteworthy that ATP synthase-coupling factor 6 (ATP5J), which is involved in ATP synthesis-coupled proton transport [37], exhibited decreased expression in ORFV-infected cells. A total of six proteins with receptor activity were identified in ORFV-infected GSF cells. TR150, K2C1,

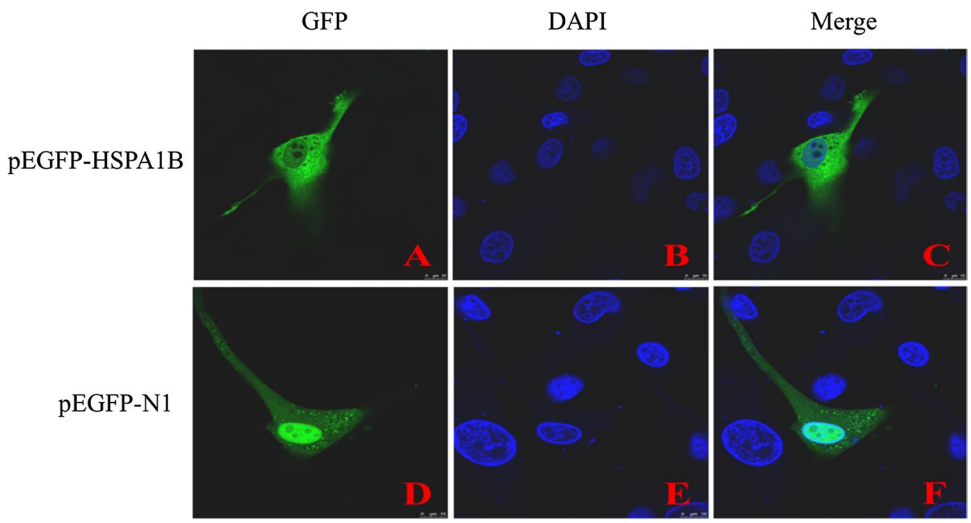

Fig. 5 The subcellular localization of HSPA1B. A monolayer of GSF cells was transfected by conventional methods using empty pEGFP-N1 as a control. Expression of the fusion protein in GSF cells was detected 18–24 h after transfection by confocal laser scanning microscopy. **A.** Green fluorescence showing the location of pEGFP-HSPA1B. **B.** Nuclear staining of pEGFP-HSPA1B. C. Merged image of panels A and B. D. Green fluorescence showing the location of pEGFP-N1. E. Nuclear staining of pEGFP-N1. F. Merged image of panels D and E

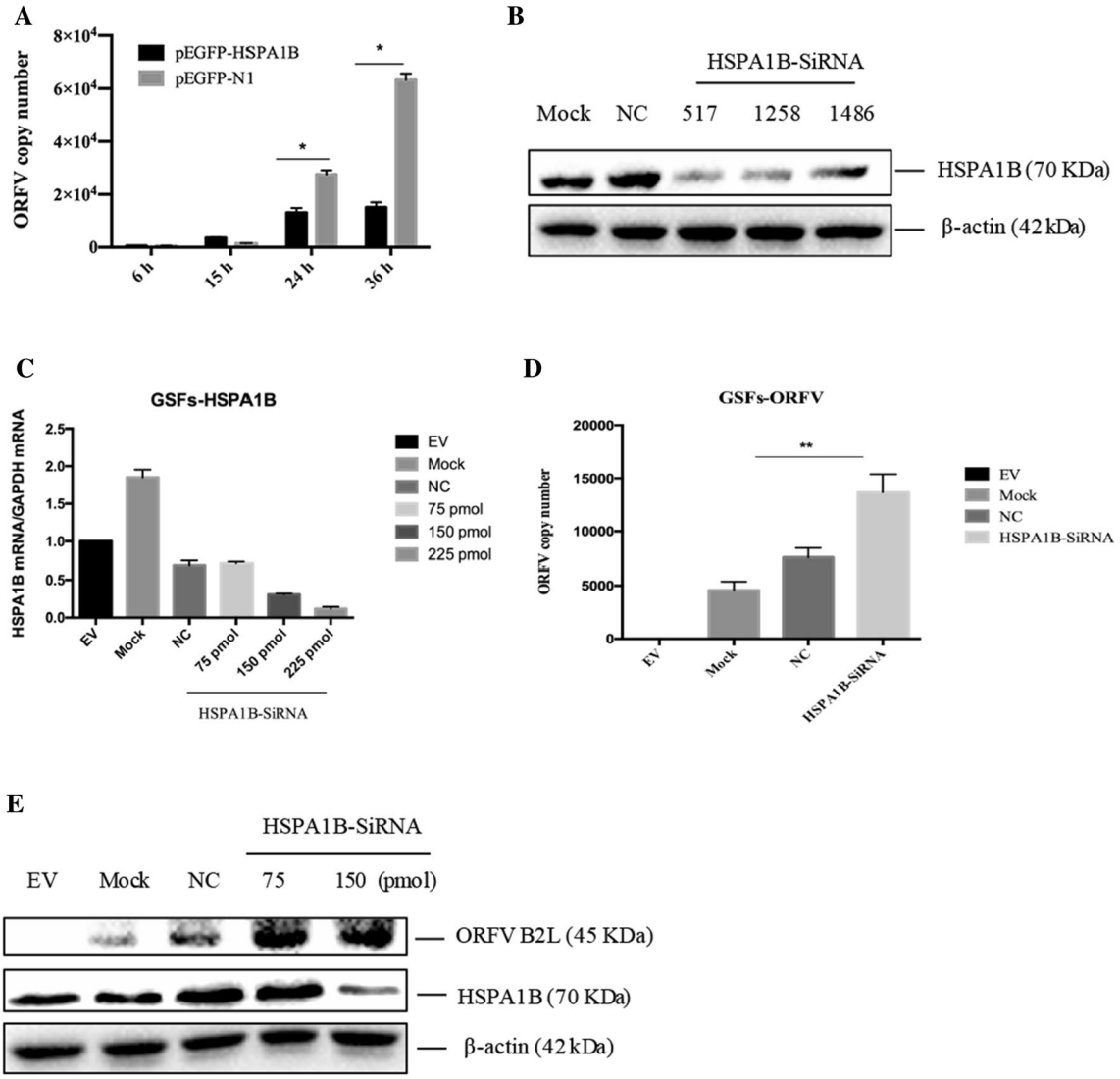

Fig. 6 HSPA1B inhibits ORFV replication. (A) Overexpression of HSPA1B suppresses ORFV replication. GSF cells were transfected with pEGFP-HSPA1B and pEGFP-N1 and infected 18 h later with ORFV at an MOI of 0.1. Cultured cells were collected at 6, 15, 24, and 36 h postinfection, and the viral DNA content was measured by RT-qPCR. (B) Evaluation of the efficiency of NC or HSPA1B siRNA in silencing HSPA1B expression. GSF cells were transfected with 150 nM HSPA1B siRNA or NC, and the expression of HSPA1B mRNA or protein was detected by Western blotting. (C-E) Down-regulation of HSPA1B promotes ORFV replication. GSF cells were transfected with NC siRNA or HSPA1B siRNA and subsequently infected with equal amounts of ORFV at an MOI of 0.1. The expression of HSPA1B and viral mRNA or protein was detected by RT-qPCR or Western blotting

SUCR1, MPRI, O10AG, and TKT were upregulated. Transketolase (TK) catalyzes several reactions in the non-oxidative branch of the pentose phosphate pathway (PPP) and serves as a bridge between the oxidative part of the PPP and the oxidative decarboxylation of glucose [17]. Recently, it has been reported that TK and its cofactor thiamine have a very high growth control coefficient. TR150 has been shown to be involved in pre-mRNA splicing and was previously believed to participate in transcriptional co-activation via its association with the TRAP complex. However, studies have not shown TR150 to be a subunit of a stable mediator complex [16, 20]. K2C1 may regulate the activity of kinases, such as PKC and SRC via binding to integrin beta-1 (ITB1) and the receptor of activated protein kinase C (RACK1/GNB2L1). Additionally, it can form a complex with C1QBP, which is a high-affinity receptor for kininogen-1/HMWK. The functions of these proteins in infected host cells are not well understood.

HSPA1B is a member of the HSP70 family. The expression level of HSP70 rapidly increases in response to cellular stresses (e.g., heat shock) or in response to certain viral infections [4, 21, 24, 26]. Genetic variations in HSP70 have

been found to be associated with individual susceptibility to several diseases by alterations in protein expression and/or function. Studies have shown that HSPs may play a significant role in virus-host cell interactions during viral infection in vivo and in vitro [1, 31]. HSP70 stabilizes proteins against aggregation and mediates the folding of newly translated polypeptides in the cytosol, as well as within organelles. It can bind with nucleotides via an ATP-dependent process and is involved in the response to stress as well as in cell apoptosis. HSP70 is associated with membrane microdomains (lipid rafts) in response to dengue virus infection and acts as a receptor complex in human cell lines and in monocytes/macrophages that are susceptible to dengue virus (DENV) infection [32]. Therefore, we hypothesize that the increased expression level of HSP70 protein may play a substantial role in the replication of ORFV. In the present study, the recombinant plasmid construct pEGFP-HSPA1B transiently expressed in GSF cells and was found to be localized in the cytoplasm. Interestingly, it has been reported that HSP70 and HSP90 are clustered around CD14, preventing them from interacting with DENV, when monocytes are incubated with "lipopolysaccharide" prior to DENV infection [32]. Our results offer an explanation for this finding. To study the effects of ORFV on cell proliferation and HSPA1B expression, GSF cells overexpressing the HSPA1B protein were infected with ORFV and viral proliferation was assessed. The results suggested that HSPA1B inhibits proliferation of ORFV in GSF cells, and this appears to occur in the middle of the viral replication cycle. Furthermore, ORFV replication was significantly enhanced in HSPA1B knockdown cells, again suggesting that HSPA1B plays an important role in ORFV-infected GSF cells. Importantly, animals are not protected against ORFV reinfections, which may be in part due to short-lived ORFV-specific adaptive immunity. Poxviruses encode a considerable number of gene products that allow them to evade the host immune response [35]. These evasive strategies may play a major role in supporting ORFV replication and allowing ORFV reinfections to occur.

Acknowledgements This study was supported by the National Key R&D Program of China (2018YFD0502100). The authors would like to thank the anonymous editors and reviewers for their valuable comments and suggestions, which helped to improve the quality of this manuscript.

References

1. Braga ACS, Carneiro BM, Batista MN, Akinaga MM, Bittar C, Rahal P (2017) Heat shock proteins HSPB8 and DNAJC5B have HCV antiviral activity. PLoS ONE 12:e0188467
2. Carbon S, Ireland A, Mungall CJ, Shu S, Marshall B, Lewis S, Ami GOH, Web Presence Working G (2009) AmiGO: online access to ontology and annotation data. Bioinformatics 25:288–289
3. Carvalho RN, Lettieri T (2011) Proteomic analysis of the marine diatom *Thalassiosira pseudonana* upon exposure to benzo(a)pyrene. BMC Genom 12:159
4. Cheung RK, Dosch HM (1993) The growth transformation of human B cells involves superinduction of hsp70 and hsp90. Virology 193:700–708
5. Chittur S, Parr B, Marcovici G (2011) Inhibition of inflammatory gene expression in keratinocytes using a composition containing carnitine, thioctic Acid and saw palmetto extract. Evid Based Complement Alternat Med 2011:985345
6. de Parseval A, Lerner DL, Borrow P, Willett BJ, Elder JH (1997) Blocking of feline immunodeficiency virus infection by a monoclonal antibody to CD9 is via inhibition of virus release rather than interference with receptor binding. J Virol 71:5742–5749
7. Deane D, McInnes CJ, Percival A, Wood A, Thomson J, Lear A, Gilray J, Fleming S, Mercer A, Haig D (2000) Orf virus encodes a novel secreted protein inhibitor of granulocyte-macrophage colony-stimulating factor and interleukin-2. J Virol 74:1313–1320
8. Dohner K, Sodeik B (2005) The role of the cytoskeleton during viral infection. Curr Top Microbiol Immunol 285:67–108
9. Duan C, Liao M, Wang H, Luo X, Shao J, Xu Y, Li W, Hao W, Luo S (2015) Identification, phylogenetic evolutionary analysis of GDQY orf virus isolated from Qingyuan City, Guangdong Province, southern China. Gene 555:260–268
10. Fleming SB, Haig DM, Nettleton P, Reid HW, McCaughan CA, Wise LM, Mercer A (2000) Sequence and functional analysis of a homolog of interleukin-10 encoded by the parapoxvirus orf virus. Virus Genes 21:85–95
11. Haig DM, Fleming S (1999) Immunomodulation by virulence proteins of the parapoxvirus orf virus. Vet Immunol Immunopathol 72:81–86
12. Haig DM (2001) Subversion and piracy: DNA viruses and immune evasion. Res Vet Sci 70:205–219
13. Haig DM, McInnes CJ (2002) Immunity and counter-immunity during infection with the parapoxvirus orf virus. Virus Res 88:3–16
14. Han B, Chen S, Dai S, Yang N, Wang T (2010) Isobaric tags for relative and absolute quantification- based comparative proteomics reveals the features of plasma membrane-associated proteomes of pollen grains and pollen tubes from *Lilium davidii*. J Integr Plant Biol 52:1043–1058
15. Hare NJ, Solis N, Harmer C, Marzook NB, Rose B, Harbour C, Crossett B, Manos J, Cordwell SJ (2012) Proteomic profiling of Pseudomonas aeruginosa AES-1R, PAO1 and PA14 reveals potential virulence determinants associated with a transmissible cystic fibrosis-associated strain. BMC Microbiol 12:16
16. Heyd F, Lynch KW (2010) Phosphorylation-dependent regulation of PSF by GSK3 controls CD45 alternative splicing. Mol Cell 40:126–137
17. Horecker BL (2002) The pentose phosphate pathway. J Biol Chem 277:47965–47971
18. Hosamani M, Scagliarini A, Bhanuprakash V, McInnes CJ, Singh RK (2009) Orf: an update on current research and future perspectives. Expert Rev Anti Infect Ther 7:879–893
19. Kurzeder C, Koppold B, Sauer G, Pabst S, Kreienberg R, Deissler H (2007) CD9 promotes adeno-associated virus type 2 infection of mammary carcinoma cells with low cell surface expression of heparan sulphate proteoglycans. Int J Mol Med 19:325–333
20. Lee KM, Hsu Ia W, Tarn WY (2010) TRAP150 activates pre-mRNA splicing and promotes nuclear mRNA degradation. Nucleic Acids Res 38:3340–3350
21. Lefeuvre A, Contamin H, Decelle T, Fournier C, Lang J, Deubel V, Marianneau P (2006) Host-cell interaction of attenuated and wild-type strains of yellow fever virus can be differentiated at early stages of hepatocyte infection. Microbes Infect 8:1530–1538

22. Li X, Shang B, Li YN, Shi Y, Shao C (2019) IFNgamma and TNFalpha synergistically induce apoptosis of mesenchymal stem/stromal cells via the induction of nitric oxide. Stem Cell Res Ther 10:18
23. Li Z, Zhang Q, Zhang Q, Xu M, Qu Y, Cai X, Lu L (2016) CXCL6 promotes human hepatocyte proliferation through the CXCR1-NFkappaB pathway and inhibits collagen I secretion by hepatic stellate cells. Biochem Cell Biol 94:229–235
24. Liao WJ, Fan PS, Fu M, Fan XL, Liu YF (2005) Increased expression of 70 kD heat shock protein in cultured primary human keratinocytes induced by human papillomavirus 16 E6/E7 gene. Chin Med J (Engl) 118:2058–2062
25. Lyttle DJ, Fraser KM, Fleming SB, Mercer AA, Robinson AJ (1994) Homologs of vascular endothelial growth factor are encoded by the poxvirus orf virus. J Virol 68:84–92
26. Mayer MP (2005) Recruitment of Hsp70 chaperones: a crucial part of viral survival strategies. Rev Physiol Biochem Pharmacol 153:1–46
27. McKeever DJ, Jenkinson DM, Hutchison G, Reid HW (1988) Studies of the pathogenesis of orf virus infection in sheep. J Comp Pathol 99:317–328
28. Mercer AA, Fleming SB, Ueda N (2005) F-box-like domains are present in most poxvirus ankyrin repeat proteins. Virus Genes 31:127–133
29. Naing A, Infante JR, Papadopoulos KP, Chan IH, Shen C, Ratti NP, Rojo B, Autio KA, Wong DJ, Patel MR, Ott PA, Falchook GS, Pant S, Hung A, Pekarek KL, Wu V, Adamow M, McCauley S, Mumm JB, Wong P, Van Vlasselaer P, Leveque J, Tannir NM, Oft M (2018) PEGylated IL-10 (Pegilodecakin) induces systemic immune activation, CD8(+) T cell invigoration and polyclonal T cell expansion in cancer patients. Cancer Cell 34:775–791.e773
30. Radtke K, Dohner K, Sodeik B (2006) Viral interactions with the cytoskeleton: a hitchhiker's guide to the cell. Cell Microbiol 8:387–400
31. Rathore AP, Haystead T, Das PK, Merits A, Ng ML, Vasudevan SG (2014) Chikungunya virus nsP3 & nsP4 interacts with HSP-90 to promote virus replication: HSP-90 inhibitors reduce CHIKV infection and inflammation in vivo. Antiviral Res 103:7–16
32. Reyes-Del Valle J, Chavez-Salinas S, Medina F, Del Angel RM (2005) Heat shock protein 90 and heat shock protein 70 are components of dengue virus receptor complex in human cells. J Virol 79:4557–4567
33. Ross PL, Huang YN, Marchese JN, Williamson B, Parker K, Hattan S, Khainovski N, Pillai S, Dey S, Daniels S, Purkayastha S, Juhasz P, Martin S, Bartlet-Jones M, He F, Jacobson A, Pappin DJ (2004) Multiplexed protein quantitation in *Saccharomyces cerevisiae* using amine-reactive isobaric tagging reagents. Mol Cell Proteomics 3:1154–1169
34. Savory LJ, Stacker SA, Fleming SB, Niven BE, Mercer AA (2000) Viral vascular endothelial growth factor plays a critical role in orf virus infection. J Virol 74:10699–10706
35. Seet BT, Johnston J, Brunetti CR, Barrett JW, Everett H, Cameron C, Sypula J, Nazarian SH, Lucas A, McFadden G (2003) Poxviruses and immune evasion. Annu Rev Immunol 21:377–423
36. Sijts A, Sun Y, Janek K, Kral S, Paschen A, Schadendorf D, Kloetzel PM (2002) The role of the proteasome activator PA28 in MHC class I antigen processing. Mol Immunol 39:165–169
37. Tezara W, Mitchell V, Driscoll S, Lawlor D (1999) Water stress inhibits plant photosynthesis by decreasing coupling factor and ATP. Nature 401:914–917
38. Wang R, Wang Y, Liu F, Luo S (2019) Orf virus: A promising new therapeutic agent. Rev Med Virol 29:e2013
39. Wilf NM, Reid AJ, Ramsay JP, Williamson NR, Croucher NJ, Gatto L, Hester SS, Goulding D, Barquist L, Lilley KS, Kingsley RA, Dougan G, Salmond GP (2013) RNA-seq reveals the RNA binding proteins, Hfq and RsmA, play various roles in virulence, antibiotic production and genomic flux in Serratia sp. ATCC 39006. BMC Genom 14:822
40. Wise LM, Veikkola T, Mercer AA, Savory LJ, Fleming SB, Caesar C, Vitali A, Makinen T, Alitalo K, Stacker SA (1999) Vascular endothelial growth factor (VEGF)-like protein from orf virus NZ2 binds to VEGFR2 and neuropilin-1. Proc Natl Acad Sci USA 96:3071–3076
41. Wisniewski JR, Zougman A, Mann M (2009) Combination of FASP and StageTip-based fractionation allows in-depth analysis of the hippocampal membrane proteome. J Proteome Res 8:5674–5678
42. Zhu Z, Wang G, Yang F, Cao W, Mao R, Du X, Zhang X, Li C, Li D, Zhang K, Shu H, Liu X, Zheng H (2016) Foot-and-Mouth Disease Virus Viroporin 2B Antagonizes RIG-I-mediated antiviral effects by inhibition of its protein expression. J Virol 90:11106–11121
43. Zou W, Ke J, Zhang A, Zhou M, Liao Y, Zhu J, Zhou H, Tu J, Chen H, Jin M (2010) Proteomics analysis of differential expression of chicken brain tissue proteins in response to the neurovirulent H5N1 avian influenza virus infection. J Proteome Res 9:3789–3798